

# Multi-Carrier Modulation: An Evolution from Time-Frequency Domain to Delay-Doppler Domain

Hai Lin,<sup>Senior Member, IEEE</sup>, Jinhong Yuan,<sup>Fellow, IEEE</sup>, Wei Yu,<sup>Fellow, IEEE</sup>,  
Jingxian Wu,<sup>Senior Member, IEEE</sup>, Lajos Hanzo,<sup>Life Fellow, IEEE</sup>

**Abstract**—The recently proposed orthogonal delay-Doppler division multiplexing (ODDM) modulation, on which is based on the new delay-Doppler (DD) domain orthogonal division (DDOP), is introduced. A substantial benefit of the DDOP-based ODDM or general ODDM Doppler domain multi-carrier (DDMC) modulation (DDMC) achieves better orthogonality with respect to the fine time and frequency resolutions of the DD domains. We first revisit the family of wireless channel models conceived for linear time varying (LTI) channels and then reviewing the conventional multi-carrier (MC) modulation schemes and their MC design guidelines for both linear time invariant (LTI) and LTV channels. Then we discuss the time-varying property of the LTV channels in DD domain impulsive response and propose an impulse function-based transmission strategy for equivalent sampled DD-domain (ESDD) channels. Next we take an in-depth look in the DDOP and the corresponding ODDM modulation to unveil DD unique infinite output relating ODDM transmission over ESDD channels. Then we point out that the conventional MC and ESDD design guidelines based on the Welch Heisenberg (WH) frame theory can be relaxed without compromising its orthogonality or without violating the WH frame theory. More specifically, using communications system having tight bandwidth WH frame theory MC modulation signals can be designed based on the WH frame theory associated with sufficient orthogonality, which gives us the high orthogonality of the MC signal within the bandwidth and duration. This is different from the conventional MC modulation design guidelines based on the global (bi)orthogonality governed by the WH frame MC mod which corresponds to the MC signals being (bi)orthogonal across the whole RF domain. WH novel design guidelines could potentially open up opportunities for developing future waveforms required by many applications such as cognitive systems associated with high delay and/or Doppler shifts, as well as integrated sensing and communications, etc.

**Index Terms**—Multi-carrier modulation, Orthogonal frequency division multiplexing (OFDM), Doubly-selective channel, Orthogonal delay-Doppler division multiplexing (ODDM), Delay-Doppler division multi-carrier (DD), DDOP, Delay-Doppler domain orthogonal Optimal DDOP, Delay-Doppler train-stepped OFDM (DDT), Sufficient (bi)orthogonality, Global (bi)orthogonality, Welch Heisenberg uncertainty principle (WHOP), orthogonal time frequency (OTFS), (Zak) Fourier Sufficient Integrated Sensing and Communications (ISAC)

Part of this paper has been presented at the IEEE GLOBECOM 2022. Part of this paper has been presented at the IEEE GLOBECOM 2022.

H. Lin is with the Department of Electrical and Electronic Systems Engineering, Graduate School of Engineering, Osaka, Moriguchi, Sakai City, 599-8501, hlin.jpn@eecon.osaka-u.ac.jp; hai.lin@iee.org).

J. Yuan is with the School of Electrical Engineering and Telecommunications, University of New South Wales, Sydney, NSW 2052, Australia; (yuanjh@unsw.edu.au).

W. Yu is with the Edward S. Rogers Sr. Department of Electrical and Computer Engineering, University of Toronto, Toronto, Ontario, Canada; (w.yu@ece.toronto.edu).

J. Wu is with the Department of Electrical Engineering, University of Arkansas Fayetteville, Arkansas, USA; (wu@uark.edu).

L. Hanzo is with the School of Electronics and Computer Science, University of Southampton, Southampton SO17 1BJ, UK (E-mail: lh@ecs.soton.ac.uk).

Global (bi)orthogonality, INTEGRATION Heisenberg uncertainty principle, Orthogonal time frequency space (OTFS), Zak transform, Integrated sensing and communications (ISAC)

A wireless channel typically introduces both time and frequency dispersions, which correspond to the channel's frequency and time selectivity, respectively. Usually, such a doubly-selective channel can be modeled as a linear time-varying system, and it is represented by its time-varying frequency dispersion or delay-Doppler spread function

frequency and time selectivity, respectively. Usually, such a doubly-selective channel can be modeled as a linear time-varying system, and it is represented by its time-varying frequency dispersion or delay-Doppler spread function [7], a.k.a. the spreading function [2]. Within the channel's coherence time, the channel model can be simplified as a linear time-invariant system, which only has time dispersion. The channel-induced dispersions have a crucial impact on signal [2], a.k.a. the spreading function [2]. Within the channel's transmission and therefore become the primary concern in the coherence time, the channel model can be simplified design of modulation schemes.

In digital communications, a modulation technique is dispersion. The channel-induced dispersions have a crucial essentially a scheme of using *analog pulses* or mathematically impact on signal transmission and therefore become the equivalent continuous-time functions to synthesize transmit primary concern in the design of modulation schemes.

In digital communications, a modulation technique is bearing *digital symbol* drawn from a signal constellation essentially a scheme of using analog pulses or mathematically equivalent continuous-time functions to synthesize a continuous-time function, which usually is the product of a digital symbol and an analog pulse. At the receiver, demodulation is often performed first by receive filtering based on matched filters or correlators. In other words, a "symbol" is on matched filters or correlators corresponding to these analog pulses. Then, the extracted signal components are fed into a channel equalizer to recover the transmitted digital symbols. At the receiver, demodulation is often performed first by To avoid interference among the symbols and consequently receive filtering based on matched filters or correlators ease the channel equalization, it is expected that these analog pulses do not interfere with each other, if possible, even in the signal components are fed into a channel equalizer to presence of channel dispersions. As a result, (bi)orthogonal recover the transmitted digital symbols. To avoid interference among the symbols and consequently ease the channel obeying the (bi)orthogonality among themselves, lie at the very heart of modulation techniques.

Since the eigenfunctions of a linear system are orthogonal of channel dispersions. As a result, (bi)orthogonal pulses or functions and excite simple scaled system outputs, using eigenfunctions, which prevent mutual interference upon obeying functions as the pulses for signal transmission seems to be an ideal strategy. For LTI systems, the eigenfunctions as the pulses for signal transmission seems to be the (bi)orthogonality among themselves, lie at the very ideal strategy. For LTI systems, the eigenfunctions are complex sinusoids with infinite duration [2], while any practical pulse

Since the eigenfunctions of a linear system are orthogonal must have a finite duration. Fortunately, complex sinusoidal functions and excite simple scaled system outputs, using periodic functions, which implies that if we choose their using eigenfunctions as the pulses for signal transmission frequencies appropriately, truncated complex sinusoids can seems to be an ideal strategy. For LTI systems, the eigenfunctions are complex sinusoids with infinite duration [2], input-output relation. The corresponding modulation scheme while any practical pulse must have a finite duration. For conceived for LTI channels is the popular time-frequency domain multi-carrier modulation, typically, the orthogonal frequency division multiplexing [2], [3], [4], [5], which has truncated complex sinusoids can still be orthogonal to each other and exhibit a scalar system input-output relation. MC modulation is a general term, while the OFDM is a special form of The corresponding modulation scheme conceived for LTI

## ACRONYMS

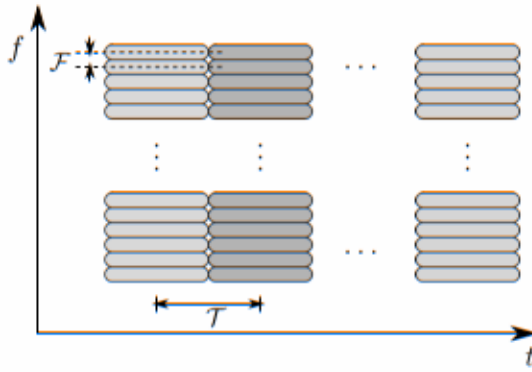


Fig. 1. TF grid in MC modulation

channels is the popular time-frequency domain multi-carrier modulation, typically the orthogonal frequency division multiplexing [2], [2], [2], [21], which has been the fifth generation mobile communication system [2], and widely adopted in wireless standards, such as the Wi-Fi [2], [2] the fourth generation mobile communication system [2], the fifth generation mobile communication system [2]. In OFDM, to achieve eigenfunction-based transmission, the transmit pulses are exactly complex sinusoids termed as subcarriers and truncated by a common time-domain window

In OFDM, to achieve eigenfunction-based transmission function named as *prototype pulse* [2]. Therefore, a popular way of thinking about the transmit pulses in the MC modulation schemes is to treat them as TF-shifted prototype pulses along a TF grid. In fact, MC modulation can be defined by a popular way of thinking about the transmit pulses in the its prototype pulse and TF grid parameterized by a specific frequency resolution (subcarrier spacing)  $F$  and a specific time window function named as *prototype pulse* [2]. Therefore, among these pulses may be quantified by the joint time-frequency resolution given as  $R = T/F$ . An example of the TF grid in MC modulation is shown in Fig. ??, where each color block presents a transmit pulse obtained by TF-shifting the prototype pulse. Given  $T$  and  $F$ , as  $R = T/F$ .

An example of the TF grid in MC modulation is shown in Fig. ??, where each color block presents a transmit pulse structure and the signal (energy) localization of the MC obtained by TF-shifting the prototype pulse. Given  $T$  and  $F$ , the two-dimensional TF domain in Fig. ?? is a gridded modulation scheme becomes that of finding the (bi)orthogonal two-dimensional domain dedicated for representing the prototype pulse with respect to  $T$  and  $F$ . Traditionally, the discrete TF structure and the signal (energy) localization transmit pulses in Fig. ?? are considered as a Wely-Heisenberg of the MC modulation. Then, the fundamental issue of designing an MC or Gabor function set [2], which is the principal tool of designing an MC modulation scheme becomes that of finding the (bi)orthogonal prototype pulse with respect to  $T$  and  $F$ . According to the WH frame theory, the (bi)orthogonal WH function sets only exist for  $R \geq 1$  [2], [2], and therefore most MC modulation schemes are designed for  $R \geq 1$  [2], [2]. Things become more complicated when the channel's frequency dispersion is significant, for example, for an LTV channel, WH function sets only exist for  $R \geq 1$  [2], [2], and therefore most MC modulation schemes are designed for  $R \geq 1$  [2]. To ease the pulse design, the underspread LTV channels at best have of MC modulation is a general term, while the OFDM is a special case of MC modulation [2].

depend on the spreading or scattering function of the channel [2]. This fact, these approximate eigenfunctions require not only frequency dispersive prototype pulses, but also a coarser LTV channel than that of the classic OFDM [21]. The channel dependency and the constraint of the channel make it impractical to realize eigenfunction-based transmission over LTV channels. The unRecepted delay-Doppler domain is modulated structured including the popular eigenfunction with frequency spacing the spreading or orthogonal defining Doppler of diversity in a multiplexing fact. These have been a propagation factor addressed the challenges of channel design for OFDM type double-selective channels. The selection of the channel is based on the channel model of OFDM channel [2]. The channel model of the LTV channel is based on the LTV channel model. The LTV channel model is approximately constant, as compared to their coherence time over which the TF state is approximately constant [2]. Although the channel's TV-CIR still needs a large number of orthogonal time-frequency space [2], [2] the channel's TV-CIR still needs a large number of orthogonal time-frequency space [2]. The DD spread function becomes deterministic and has a compact representation relying on DD parameters. Since each propagation path imposes DD domain attenuation and delay but also the Doppler spread, the LTV-CIR of an LTV channel is longer than the superposition of paths with complex sinusoids associated with Doppler frequencies and therefore presents fading. On the other hand, its DD spread function is apparently characterized by each path's attenuation, delay and Doppler. Then, the destructive multi-path fading exhibited by the TV-CIR turns DD spread function becomes DD domain, where path diversity can be harvested as a benefit of independent paths [2]. Based on these observations, the DD domain modulation schemes aim for coupling [2] the modulated signal with the DD domain channel, equivalently with the superposition of path-wise complex sinusoids. Here, coupling represents the matches between the TF grid, namely fading. On the other hand, DD signal and those of simply channel [2]. Given an ideal coupling, delay and Doppler, the DD domain channels can be exploited to obtain diversity gains with separable paths in the DD domain, where path diversity can be harvested as a benefit of independent complexity [2]. Based on these observations, the DD domain modulation scheme coupling the fundamental mismatched DD signal with the DD domain also resides in the pulse design with the DD approach function with channel coupling [2]. With matched resolutions, the DD domain between modulated TF grid and localized pulses in the DD domain. However, such a delay-Doppler DD domain localized pulse could violate the Heisenberg uncertainty and sparsity and DD domain does not exist. To be exploited this obtain diversity gains with digital DD domain symbol, and the digital TF domain signals via an inverse symplectic finite

<sup>2</sup>Although the term of stationary time was originally used in the stationary modeling of LTV channels, where originally it is a stationary time over which LTV channel's delay and Doppler shifts remain almost the same.

Fourier achieves form disable digital purification. Then it is allowed pilot the channel pulse slow with pre-TF scaling gain implemented to carry these pre-coded signals and synthesize a conventional time-frequency of DDD in multi-carrier modulation away from the pulse design. In this case, to achieve the transmit signature of OTFS coupling with the time-frequency resolution in the DD domain, the modulation OTFS requires a localized pre-coded OFDM domain. In OTFS, the ideal pulse delay-Doppler domain localization pulse around the channel induced delay and Doppler is unfortunately, and the channel pulse does not exist either [2]. As some of the TFQPSK can meet this digital DDD domain while the widely adopted TFQPSK angular prototype pulse in popular QPSK, QPSK, FOFPSK, TEOP, and therefore not ideal, which will face practical challenges in implementation such as high power of burst emission and severe interference and synthesize a conventional time-frequency domain. On the other hand, based on the newly discovered delay-Doppler domain orthogonal pulses, ODDM or DDOP presents a novel time-frequency domain multi-carrier modulation scheme that can avoid all the impediments of OTFS. In OTFS, above all, Note that the time (duration) and frequency (bandwidth) constraints in any practical TD-Doppler domain region of interests, which does not exist either [2], as none of the TEOPs equivalent to the requirement. Meanwhile, the channel adopts orthogonal basis prototype delay and Doppler pulses of OTFS [2]; it is still a TFOP and therefore non-ideal, which will face practical challenges in system realization, a gridded high DD domain whose grid and resolution are defined by the delay and Doppler resolutions.

On the other hand, based on the newly discovered delay-Doppler domain orthogonal pulse, ODDM represents a novel delay-Doppler domain multi-carrier modulation scheme that can avoid the impediment of OTFS mentioned above [2]. Note that the time (duration) and frequency (bandwidth) constraint of frequency resolution, a DD domain demodulation region is naturally multi-carrier moduation, which requires a DDLP or a DDOP. Although the DDLP [1] an equivalent sampled delay-Doppler domain channel does not exist, the DDOP introduced in [7], [17], [1] consists of a train of square-root Nyquist pulses, and behaves like the "nonexistent" DDLP in the TF region of interests, and the DD domain in practical systems becomes a gridded DD domain whose grids are defined by the and the ESDD channel. Specifically, without violating the Heisenberg uncertainty principle, the DDOP has an equally spaced signal localization in the TF region of interests [7] to domain but with much finer resolutions, because the satisfy the orthogonality with respect to the specific delay and delay and Doppler have the physical units of time and Doppler resolutions. It should be noted that the ESDD channel frequency, respectively. According to the Heisenberg uncertainty principle, the DDOP has an equally spaced signal localization in the TF region of interests [7] to domain but with much finer resolutions, because the satisfy the orthogonality with respect to the specific delay and delay and Doppler have the physical units of time and Doppler resolutions. It should be noted that the ESDD channel frequency, respectively. The family of classic TFMC modulation schemes is reviewed in Section III and Section IV for LTV and LTI channels, respectively, focusing on their transmission strategies, pulse design guidelines based on the WH frame theory can be relaxed without compromising its orthogonality. In of classic TFMC modulation schemes is reviewed in Section particular, instead of the global (bi)orthogonality governed by the WH frame theory, the MC pulse design respectively, focusing on their transmission strategies, pulse can be redefined by exploiting the WH subset based designs and implementation methods. Then, based on the sufficient (bi)orthogonality. This new interpretation of continuous-time channel IO relation. Section V investigates the sufficient (bi)orthogonality actually relaxes the JTFR properties of the ESDD channel, clarifies the corresponding constraint of  $R > 1$  for (bi)orthogonal pulse design and time-varying DD domain impulse response, and proposes an leads to more general DDMM modulation schemes. This impulse function based transmission strategy. The DDOP and novel design guideline may open up opportunities for its (bi)orthogonality are analyzed in details in Section VI, developing future waveforms required by new applications where the relation to the WH frame theory is explained and such as integrated communications and sensing, high-new pulse design guidelines are proposed. The important properties of the ODDM modulation are unveiled in Section VII, including its signal localization, bandwidth efficiency, implementation methods, and ISAC potentials. Our simulation results are provided in Section VIII and finally Section IX concludes the paper.

The rest of the paper is organized as follows: Section II revisits the LTV and LTI channel models, especially the ESDD channel model taking into account the time and frequency constraints of practical signal waveforms. The family of classic TFMC modulation schemes is reviewed in Section III and Section IV for LTV and LTI channels, respectively, focusing on their transmission strategies, pulse design guidelines based on the WH frame theory can be relaxed without compromising its orthogonality. In particular, instead of the global (bi)orthogonality governed by the WH frame theory, the MC pulse design respectively, focusing on their transmission strategies, pulse can be redefined by exploiting the WH subset based designs and implementation methods. Then, based on the sufficient (bi)orthogonality. This new interpretation of continuous-time channel IO relation. Section V investigates the sufficient (bi)orthogonality actually relaxes the JTFR properties of the ESDD channel, clarifies the corresponding constraint of  $R > 1$  for (bi)orthogonal pulse design and time-varying DD domain impulse response, and proposes an leads to more general DDMM modulation schemes. This impulse function based transmission strategy. The DDOP and novel design guideline may open up opportunities for its (bi)orthogonality are analyzed in details in Section VI, developing future waveforms required by new applications where the relation to the WH frame theory is explained and such as integrated communications and sensing, high-new pulse design guidelines are proposed. The important properties of the ODDM modulation are unveiled in Section VII, including its signal localization, bandwidth efficiency, implementation methods, and ISAC potentials. Our simulation results are provided in Section VIII and finally Section IX concludes the paper.

The family of classic TFMC modulation schemes is reviewed in Section III and Section IV for LTV and LTI channels, respectively, focusing on their transmission strategies, pulse design guidelines based on the WH frame theory can be relaxed without compromising its orthogonality. In particular, instead of the global (bi)orthogonality governed by the WH frame theory, the MC pulse design respectively, focusing on their transmission strategies, pulse can be redefined by exploiting the WH subset based designs and implementation methods. Then, based on the sufficient (bi)orthogonality. This new interpretation of continuous-time channel IO relation. Section V investigates the sufficient (bi)orthogonality actually relaxes the JTFR properties of the ESDD channel, clarifies the corresponding constraint of  $R > 1$  for (bi)orthogonal pulse design and time-varying DD domain impulse response, and proposes an leads to more general DDMM modulation schemes. This impulse function based transmission strategy. The DDOP and novel design guideline may open up opportunities for its (bi)orthogonality are analyzed in details in Section VI, developing future waveforms required by new applications where the relation to the WH frame theory is explained and such as integrated communications and sensing, high-new pulse design guidelines are proposed. The important properties of the ODDM modulation are unveiled in Section VII, including its signal localization, bandwidth efficiency, implementation methods, and ISAC potentials.

Our simulation results are provided in Section VIII and finally Section IX concludes the paper.

### A. Propagation Channel Models

**Notations:** In this paper, uppercase boldface letters are used to represent complex-valued baseband signal (baseband is used for  $B/2$  column vectors in the channel),  $\Pi_T(t)$  denotes the *strictly time-limited* signal of unit energy and support  $[0, T]$  in frequency domain.  $T$  denotes the time-impulse time-limited signals having finite duration in the bandwidth  $B$ . Finally,  $\delta(\cdot, \nu)$  is the *essential sense* of ambiguity function having a duration of  $\mathcal{J}(t)$  may be considered as both time- and band-limited.

For a wireless system communicating over an LTV channel, given the carrier frequency  $f_c$ , the passband radio frequency signal  $x(t) = \Re\{x(t)e^{j2\pi f_c t}\}$  is amplified and then sent through the LTV channel. We assume that the LTV channel is composed of  $\bar{P}$  paths corresponding to  $\bar{P}$  discrete specular scatterers. Under the “channel whiteness” assumption of  $B \ll f_c$ , the variation of path attenuations and propagation delays vs. frequency can be omitted. Furthermore, noise terms are the band of  $(-\bar{B}/2, \bar{B}/2]$ . Due to its limited bandwidth, ignored in the following discussion for the sake of simplicity,  $x(t)$  cannot be strictly time-limited. Similarly, a time-limited signal cannot be strictly frequency-limited. Then, we have the received *real-valued passband signal* [?], where  $a_p(t)$  and  $\tilde{\tau}_p(t)$  are the time-varying attenuation and delay of the  $p$ -th path, respectively. The corresponding received complex-valued baseband signal  $y(t) = \Re\{y(t)e^{j2\pi f_c t}\}$  is amplified and then sent through the LTV channel. We assume that the LTV channel is composed of  $\bar{P}$  paths corresponding to  $\bar{P}$  discrete specular scatterers. Under the “narrowband” assumption of  $B \ll f_c$ , the variation of path attenuations and propagation delays vs. frequency represents the “gain” or the “attenuation” of the  $p$ -th path. Thus, the baseband TV-CIR has the same form as

$$\begin{aligned} \bar{h}(t, t) &= \sum_{p=1}^{\bar{P}} \bar{h}_p(t) \delta(t - \tilde{\tau}_p(t)), \\ y(t) &= \sum_{p=1}^{\bar{P}} a_p(t) x(t - \tilde{\tau}_p(t)), \end{aligned} \quad (1)$$

where  $\delta$  denotes the Kronecker delta function and  $t$  is the delay domain variable.

During the channel’s stationary time when the time-variation of  $\tilde{\tau}_p(t)$  accounting for delay drift can be neglected and the time variation of  $a_p(t)$  is caused by a Doppler spread  $\tilde{\nu}_p$  [?], we have  $\tilde{\tau}_p(t) = \bar{y}(t) + \sum_{p=1}^{\bar{P}} \bar{h}_p(t) x(t) e^{j2\pi \tilde{\nu}_p t}$ . Then, we can rewrite the received complex-valued baseband signal in (??) as

where  $\bar{h}_p(t) = a_p(t) e^{-j2\pi f_c \tilde{\tau}_p(t)}$  represents the “gain” or the attenuation of the  $p$ -th path. Thus, the baseband TV-CIR can be written as

$$\bar{h}(t, t) = \sum_{p=1}^{\bar{P}} \bar{h}_p e^{j2\pi \tilde{\nu}_p t} \delta(t - \tilde{\tau}_p), \quad (3)$$

where  $\delta$  denotes the Kronecker delta function and  $t$  is the delay domain variable.

<sup>3</sup>The bandwidth may be defined by ignoring the negligible high-frequency tails beyond  $[-\bar{B}/2, \bar{B}/2]$ .

During spreading and DD’s stationary representation of the time-variation of  $\tilde{\tau}_p(t)$  accounting for “delay drift” can be neglected and the time variation of  $a_p(t)$  is caused by a Doppler spread  $\tilde{\nu}_p$  [?]. We have  $\tilde{\tau}_p(t) = \tilde{\tau}_p + \tilde{\nu}_p t$  and  $\bar{h}_p(t) = \bar{h}_p e^{j2\pi \tilde{\nu}_p t}$ . Then, we can rewrite the received complex-valued baseband signal in (??) as

$$\begin{aligned} \bar{h}(t) &= \sum_{p=1}^{\bar{P}} \bar{h}_p \delta(t - \tilde{\tau}_p), \\ \bar{h}(\tau, t) &= \sum_{p=1}^{\bar{P}} \bar{h}_p e^{j2\pi \tilde{\nu}_p t} \delta(t - \tilde{\tau}_p), \end{aligned} \quad (4)$$

which only introduces time dispersion. The IO relation of the channel coding DD’s domain representation of the LTV variation between  $x(t)$  and the time-invariant impulse response  $\bar{h}(\tau)$  in (??), given by

$$\bar{h}(\tau, \nu) = \sum_{p=1}^{\bar{P}} \bar{h}_p \delta(\tau - \tilde{\tau}_p) \delta(\nu - \tilde{\nu}_p), \quad (6)$$

$$y(t) = \sum_{p=1}^{\bar{P}} \bar{h}_p x(t - \tilde{\tau}_p) = \int_{-\infty}^{\infty} x(t - \tau) \bar{h}(\tau) d\tau. \quad (8)$$

where  $\nu$  is the Doppler domain variable.

During the coherence time, when the channel’s time-variation caused by  $\tilde{\nu}_p$  can be further neglected, (??) becomes our familiar LTI channel’s impulse response and the baseband TV-CIR in (??) as

$$\bar{h}(\tau) = \sum_{p=1}^{\bar{P}} \bar{h}_p \delta(\tau - \tilde{\tau}_p), \quad (7)$$

$$\bar{h}(\tau, t) = \sum_{p=1}^{\bar{P}} \bar{h}_p e^{j2\pi \tilde{\nu}_p t} \delta(\tau - \tilde{\tau}_p). \quad (5)$$

which only introduces time dispersion. The IO relation of the channel coding DD’s domain representation of the LTV variation between  $x(t)$  and the time-invariant impulse response  $\bar{h}(\tau)$  in (??), given by

$$\bar{h}(\tau, \nu) = \sum_{p=1}^{\bar{P}} \bar{h}_p \delta(\tau - \tilde{\tau}_p) \delta(\nu - \tilde{\nu}_p), \quad (6)$$

$$y(t) = \sum_{p=1}^{\bar{P}} \bar{h}_p x(t - \tilde{\tau}_p) = \int_{-\infty}^{\infty} x(t - \tau) \bar{h}(\tau) d\tau. \quad (8)$$

During the two-dimensional discrete function in the DD-domain,  $\bar{h}(\tau, \nu)$  in (??) represents a deterministic channel model and it is known as a special case of the spreading function  $\mathcal{S}(\tau, \nu)$ , which usually is a 2D continuous function characterizing a continuum of scatterers [?]. The counterpart of the spreading function  $\mathcal{S}(\tau, \nu)$  in the statistical description of LTV channel is the scattering function given by [?], which only introduces time dispersion. The IO relation of the LTI channel  $\bar{h}(\tau, \nu)$  in (??) exactly (written as a one-dimensional convolution between  $x(t)$  and the time-invariant impulse response  $\bar{h}(\tau)$  in (??)) given, by

When  $\mathcal{C}(\tau, \tilde{\tau}, \nu, \tilde{\nu}) = \mathcal{C}(\tau, \nu) \delta(\tilde{\tau} - \tau) \delta(\tilde{\nu} - \nu)$ , we obtain the well-known wide-sense stationary uncorrelated scattering channel. In this paper, we assume that communications occur in the stationary time interval with a deterministic channel model represented by the spreading function, instead of a random LTV channel model represented function in the DD-domain.  $\bar{h}(\tau, \nu)$  in (??) represents a deterministic channel model and general spreading spectrum case of the spreading function, when a signal is a 2D can be generalized characterizing a continuum of scatterers [?]. The counterpart of the spreading function  $\mathcal{S}(\tau, \nu)$  in the statistical description of LTV channel is the scattering function given by [?], whose frequency-domain representation is

$$\mathcal{L}(\tau, \tilde{\tau}, \nu, \tilde{\nu}) = \mathbb{E} \{ \mathcal{S}(\tau, \nu) \mathcal{S}^*(\tilde{\tau}, \tilde{\nu}) \}. \quad (9)$$

$$Y(f) = \int_{-\infty}^{\infty} \int_{-\infty}^{\infty} \mathcal{S}(\tau, \nu) X(f - \nu) e^{-j2\pi \tau(f - \nu)} d\tau d\nu. \quad (11)$$

When  $\mathcal{C}(\tau, \tilde{\tau}, \nu, \tilde{\nu}) = \mathcal{C}(\tau, \nu) \delta(\tilde{\tau} - \tau) \delta(\tilde{\nu} - \nu)$ , we obtain the well-known wide-sense stationary uncorrelated scattering channel. In this paper, we assume that communications occur in the stationary time interval with a deterministic channel model represented by the spreading function, instead of a random LTV channel model represented by an ensemble of spreading functions.

Given a general spreading function  $\mathcal{S}(\tau, \nu)$ , the received complex-valued baseband signal in (??) can be generalized to  $\mathcal{S}^{(g)}(t, f) = \int_{-\infty}^{\infty} \int_{-\infty}^{\infty} \mathcal{S}(\tau, \nu) X^{(g)}(t - \tau, f - \nu) e^{-j2\pi \tau(f - \nu)} d\tau d\nu$ . Then, the STFT of the received signal  $y(t)$  becomes [?]

$$y(t) = \int_{-\infty}^{\infty} \int_{-\infty}^{\infty} \mathcal{S}(\tau, \nu) x(t - \tau) e^{j2\pi \nu t} d\tau d\nu, \quad (10)$$

whose frequency-domain representation is

$$Y(f) = \int_{-\infty}^{\infty} \int_{-\infty}^{\infty} S(\tau, \nu) X^{(Analog)}(f-\nu) e^{-j2\pi(f-\nu)\tau} d\tau d\nu \quad (11)$$

Meanwhile, given a normalized analysis window  $g(t)$ , the STFT of the transmitted signal  $x(t)$  is defined as

$$X^{(g)}(f) = \int_{-\infty}^{\infty} \int_{-\infty}^{\infty} x(t) g^*(t-\tau) e^{j2\pi f t} d\tau dt \quad (12)$$

Then, the STFT of the received signal  $y(t)$  becomes [?]

$$Y^{(g)}(t, f) = \int_{-\infty}^{\infty} \int_{-\infty}^{\infty} S(\tau, \nu) X^{(g)}(t-\tau, f-\nu) e^{-j2\pi(t-\tau, f-\nu)} d\tau d\nu.$$

It is interesting to observe that *except for the phase* [13] it is interesting to observe that *except for the phase term  $e^{-j2\pi(t-\tau, f-\nu)}$*  the above STFT-based IO relation of the LTV channel is a 2D convolution.

In mobile communications, the LTV channel is typically underspread with a spreading function confined to a small region in the DD domain. In particular, let  $\tau_p^{\max}$  and  $\nu_p^{\max}$  denote the small region in the DD domain. In particular, let  $\tau_p$  and  $\nu_p$  denote the channel delay spread and Doppler spread, respectively. Then, an LTV channel is said to be underspread, when  $\tau_p^{\max} \ll \tau_p$  and  $\nu_p^{\max} \ll \nu_p$ . Also, it should be noted that an LTV channel is generally *not* underspread when  $\tau_p \ll \tau_p^{\max}$  or  $\nu_p \ll \nu_p^{\max}$ . Also, it should be noted that  $\tau_p$  and  $\nu_p$  are generally off-grid and the LTV channel  $S(\tau, \nu)$  or  $h(\tau, \nu)$  is neither time- nor band-limited, as evidenced by its TF representation [?].

$$\mathcal{L}_S(t, f) = \int_{-\infty}^{\infty} \int_{-\infty}^{\infty} S(\tau, \nu) e^{j2\pi(t\tau + f\nu)} d\tau d\nu. \quad (14)$$

$$\mathcal{L}_h(t, f) = \int_{-\infty}^{\infty} \int_{-\infty}^{\infty} h(\tau, \nu) e^{j2\pi(t\tau + f\nu)} d\tau d\nu. \quad (14)$$

### B. Equivalent Sampled Channel Models

Fig. 2 illustrates the block diagram of a typical wireless communication system. A block diagram of a typical wireless communication link is shown. The link consists of a transmitter and a receiver. The transmitter includes a digital signal processor (DSP), a modulator, and an RF up-converter. The receiver includes a low-noise amplifier (LNA), a down-converter, a demodulator, and an equalizer. The channel is represented by a block labeled "Equivalent Sampled Channel". The channel is modeled as a 2D convolution of the transmitted signal and the received signal. The channel is also represented by its TF representation  $\mathcal{L}_S(t, f)$  or  $\mathcal{L}_h(t, f)$ .

is just the transmit/receive pulse. For MC modulation, the effective channel model is also valid, provided that the transmit/receive filter represents the overall effect of the subcarrierwise transmit/receive pulses/filter, for example, an ideal LPF having a passband bandwidth of  $B$ .

Note that baseband signal processing is typically conducted by digital signal processor, and therefore requires an appropriate sampling of the received baseband signal  $y(t)$ . The frequency dispersion of the LTV channel will expand the bandwidth of  $y(t)$  beyond  $B$ , but this is usually ignored in practice, since the Doppler spread is relatively small (on the order of tens to hundreds Hz) compared to the bandwidth  $B$  (on the order of MHz) [?].

For SC modulation, matched LPF pulses/letters for example, matched LPF having a passband bandwidth sampled at the symbol rate. The baseband signal processing typically is conducted by digital signal processor and therefore requires an appropriate sampling of the received baseband signal  $y(t)$ . The frequency dispersion of the LTV channel will expand the bandwidth of  $y(t)$  beyond  $B$ , but this is usually ignored in practice, since the Doppler spread is relatively small (on the order of tens to hundreds Hz) compared to the bandwidth  $B$  (on the order of MHz) [?].

For SC modulation, the LPF can act as the receive matched filter, the output of which is sampled at the symbol rate. The symbol rate (or sampling rate) is usually lower than  $B$  to implement a narrowband demodulator and then achieve zero inter-symbol-interference over the entire bandwidth. For MC modulation, the LPF acts as an anti-aliasing filter, which may be omitted if  $y(t)$  has been appropriately filtered in the phase and quadrature demodulator.

The equivalent sampled channel is implemented as a 2D convolution of the transmitted signal and the received signal. The channel is represented by its TF representation  $\mathcal{L}_S(t, f)$  or  $\mathcal{L}_h(t, f)$ . The channel is a grid signal and the sample duration  $b_p$  and the sample rate  $f_p$  are given by

$$b_p = \frac{W}{P}, \quad f_p = W/b_p, \quad (15)$$

$$\mathcal{L}_h(t, f) = \sum_{p=1}^P h_p \delta(t - t_p) \delta(f - f_p), \quad (16)$$

where we have  $P \geq \tilde{P}$ ,  $t_p = l_p/W$ ,  $f_p = k_p/T$ ,  $l_p, k_p \in \mathbb{Z}$ , and  $1/W$  (symbol rate) and  $1/T$  (symbol period) are  $\frac{W}{2}$  and  $\frac{W}{2}$  respectively. The ESDD channel is the delay and Doppler resolved DD domain corresponding to the DD domain associated with the specific delay (time) and Doppler (frequency) resolutions.

| TABLE I<br>MC MODULATION PARAMETERS |   |                  |
|-------------------------------------|---|------------------|
| Digital SymNotation                 | Analog WParamter  | RF Up-conversion |
| $\mathcal{F}$                       | Baseband Modulation frequency resolution, subcarrier spacing, fundamental frequency | $x(t)$           |
| $T$                                 | symbol period, $T = 1/\mathcal{F}$  |                  |
| $\mathcal{T}$                       | time Sampling   |                  |
| $R$                                 | Analog in   |                  |
| $N$                                 | Demodulator/Equalizer   |                  |
| $M$                                 | number of subcarriers   |                  |
| $g(t)$                              | transmit prototype pulse  |                  |
| $G(f)$                              | Fourier transform of $g(t)$   |                  |
| $B_g$                               | bandwidth of $g(t)$ , span of $G(f)$  |                  |
| $\gamma(t)$                         | receive prototype pulse   |                  |

Fig. 2. Block diagram of a duration of MC modulation

TABLE I  
MC Modulation Parameters

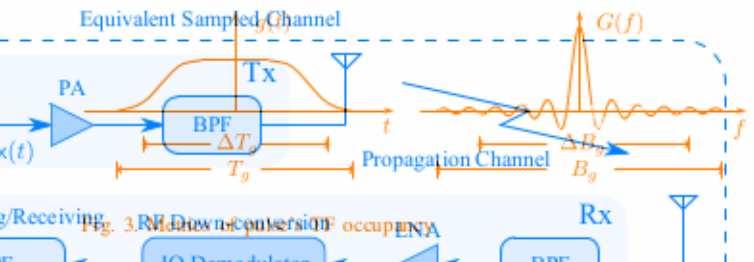


Fig. 3. RF Down-conversion occupies ENA

| Notation      | Parameter  |
|---------------|--|
| $\mathcal{F}$ | frequency resolution, subcarrier spacing, fundamental frequency                          |
| $T$           | $L_h(t, f) = \sum_p h_p e^{j2\pi(\mathcal{F}p - f)t}$ symbol period, $T = 1/\mathcal{F}$ |
| $\mathcal{T}$ | time resolution, symbol interval   |
| $\mathcal{R}$ | JTFR, $\mathcal{R} = \mathcal{T}\mathcal{F}$   |
| $N$           | number of subcarriers  |
| $M$           | number of symbols  |
| $g(t)$        | transmit prototype pulse duration of $g(t)$ , symbol duration                            |
| $G(f)$        | Fourier transform of $g(t)$  |
| $B_g$         | bandwidth of $g(t)$ , span of $G(f)$   |
| $\gamma(t)$   | receive prototype pulse  |

whose FD representation, i.e. the channel's transfer function is. Then the delay spread of the ESDD channel is given by  $\tau_{\max} = \tau_P$ , and the LTI version of (??) is given by (18)

$$H(f) = \sum_{p=1}^P h_p e^{-j2\pi f p}, \quad (18)$$

for  $f \in [-\frac{W}{2}, \frac{W}{2}]$ . Note that the relation between (??) and (??) can be found in [?] when the transmit filter is an ideal LPF having FDR as bandwidth of the channel's transfer function.

This impact of the LTV and the LTI channels imposed on a practical modulation waveform is characterized by the equivalent sampled channel models in (??) and (??), respectively. Bearing in mind these impacts, a modulation scheme entails an appropriate orthogonal pulse design to strike a comprise between the bandwidth efficiency and the complexity of the channel's transfer function.

Starting from 1950s, MC modulation techniques including the complexity of demodulation and equalization. In the following sections, we will discuss the modulation designs in the literature, there are many technical reviews of OFDM conceived for these channels.

The main purpose of this paper is to study the new ODDM/DDMC modulation schemes designed for LTV channels.

The main purpose of this paper is to study the new ODDM/DDMC modulation schemes designed for LTV channels.

The main purpose of this paper is to study the new ODDM/DDMC modulation schemes designed for LTV channels.

The main purpose of this paper is to study the new ODDM/DDMC modulation schemes designed for LTV channels.

is known that the (bi)orthogonal pulse design in conventional TFMC modulation schemes is closely related to the properties of a (bi)orthogonal WH function set, which is governed by the WH frame theory [?]. In this section, we will review the conventional TFMC modulation schemes in particular from the perspective of the eigenfunction-based transmission strategy, the WH frame theory based (bi)orthogonal pulse design principles, and the implementation methods. Meanwhile, the inverse of the time evolution of OFDM in [?, Table II].

The main purpose of this paper is to study the new ODDM/DDMC modulation, the corresponding new pulse design, and the unique transmission strategy for LTV channels. It is known that the (bi)orthogonal pulse design by a conventional TFMC modulation schemes is closely related to the properties of a (bi)orthogonal WH function set, which is governed by the WH frame theory [?]. In this section, we will review the conventional TFMC modulation schemes, in particular from the perspective of the eigenfunction-based transmission strategy, the WH frame theory based (bi)orthogonal pulse design principles, and the implementation methods. Meanwhile, the inverse of the time evolution of OFDM in [?, Table II].

A. Pulse Design Principles

The transmission principle of MC modulation synthesized by the transmit pulses in (??) is as follows:

MC modulation can be represented by a function set [?]

$$x(t) = \sum_{m=0}^{M-1} \sum_{n=-N/2}^{N/2} g(t-mT) e^{j2\pi n \mathcal{F}(t-mT)}, \quad (20)$$

where  $g_{m,n} \triangleq g(t-mT) e^{j2\pi n \mathcal{F}(t-mT)}$  and  $g(t)$  is the prototype pulse. Similarly, we can form the receive pulses ( $\gamma, T, \mathcal{F}$ ) using another prototype pulse  $\gamma(t)$  having the same time and frequency resolutions. Meanwhile, the inverse of the frequency resolution is known as the symbol period denoted by  $T = 1/\mathcal{F}$ .

Then the transmission principle of MC modulation synthesized by the transmit pulses in (??) is as follows:

$$x(t) = \sum_{m=0}^{M-1} \sum_{n=-N/2}^{N/2} X[m, n] g(t-mT) e^{j2\pi n \mathcal{F}(t-mT)}, \quad (20)$$

where  $g_{m,n} \triangleq g(t-mT) e^{j2\pi n \mathcal{F}(t-mT)}$  and  $g(t)$  is the prototype pulse. Similarly, we can form the receive pulses ( $\gamma, T, \mathcal{F}$ ) using another prototype pulse  $\gamma(t)$  having the same time and frequency resolutions. Meanwhile, the inverse of the frequency resolution is known as the symbol period denoted by  $T = 1/\mathcal{F}$ .

Let  $T_g$  and  $G(f)$  denote the duration and the Fourier transform of  $g(t)$ , respectively. The main parameters of MC modulation are listed in Table ??, where  $B_g$ , the bandwidth of  $g(t)$  or the span of  $G(f)$ , is also defined in an essential sense [?]. The number of MC symbols contained by  $x(t)$ , and the number of subcarriers  $N$  is usually supposed to be an even number. Furthermore,  $X[m, n]$  for  $-N/2 \leq n \leq N/2$ ,  $0 \leq m \leq M-1$  represent the information-bearing digital symbols drawn from a signal constellation diagram, for example, quadrature amplitude modulation.

Then, the transmit waveform of MC modulation synthesized by the transmit pulses in (??) is given by

$$x(t) = \sum_{m=0}^{M-1} \sum_{n=-N/2}^{N/2} X[m, n] g(t-mT) e^{j2\pi n \mathcal{F}(t-mT)}, \quad (20)$$

is attained by the Gaussian pulse [?]<sup>4</sup>. Usually,  $g(t)$  is said to be well-localized in the sense of minimum TF energy spread, when its signal energy is concentrated around its centre to have a small TFA [?].

Given  $T$  and  $\mathcal{F}$ , the fundamental issue of MC modulation is to find  $g(t)$  and  $\gamma(t)$  satisfying the orthogonal condition of Fig. 3. Metrics of pulse's TF occupancy

$$\langle g_{m,n}, g_{m,n} \rangle = \delta(m - m) \delta(n - n), \quad (21)$$

or the biorthogonal condition of

$$\langle g_{m,n}, \gamma_{m,n} \rangle = \delta(m - m) \delta(n - n). \quad (22)$$

MC modulation are listed in Table ??, where  $B_g$ , the bandwidth of  $g(t)$  in TF domain spans of a 2D phase space defined function of  $(m, n)$  of a discrete grid sampling in the phase space apart from the  $T_g$  and  $\mathcal{F}$  the sampling resolution metric of TF Occupancy  $\mathcal{R}(t)$  in the TF domain is its time-frequency area  $\Delta T_g \Delta B_g$  which is given by the inverse of the JTFR  $\Delta T_g$  and  $\mathcal{R}$  effect from band-limited theory, the existence of suborthogonal sets of the TD and FD shapings especially in [?], which can be exemplified as different cases (a) (b) (c) (d),  $T_g$ , and  $\Delta T_g$ ,  $\mathcal{R}$ ,  $B_g$  and  $\Delta B_g$  are shown in Fig. ??.

Due to the Heisenberg uncertainty principle, the TFA obeys a lower bound

$$4 > 1/(4\pi) \text{ known as the Gabor limit, which is attained by the Gaussian pulse.} \quad [?]$$

Therefore, they are not well-localized in the TF domain.

Under-critical sampling ( $\mathcal{R} < 1$ ): Neither orthogonal nor biorthogonal WH sets exist, if  $\mathcal{R}$  is sufficiently larger than 1.

Given  $T$  and  $\mathcal{F}$ , the fundamental issue of MC modulation is to find  $g(t)$  and  $\gamma(t)$  satisfying the orthogonal condition of

Critical sampling ( $\mathcal{R} = 1$ ): Orthogonal WH sets exist. However, they have either infinite TD or FD energy spread according to the Balian-Low theory [?]. Therefore, they are not well-localized in the TF domain.

Over-critical sampling ( $\mathcal{R} > 1$ ): Well-localized orthogonal or biorthogonal WH sets exist, if  $\mathcal{R}$  is sufficiently larger than 1.

Here, we define the bandwidth efficiency of the transmitted signal  $x(t)$  as

$$\eta = \frac{MN}{BT_x}. \quad (23)$$

By considering the TF domain as a 2D phase space, the function set in (??) forms a discrete grid "sampling" the phase space [?], [?], where the sampling resolution is the density of  $(g, \gamma, \mathcal{F})$  but also on the duration  $T_g$  of  $g(t)$ , JTFR  $\mathcal{R} = T_g \mathcal{F}$ . Then, the function set in (??) is treated and on the bandwidth  $B_g$  of  $g(t)$ . In other words, to achieve a WH set, the density of which is given by the inverse high bandwidth efficiency  $\mathcal{R}$ , we have to place the pulses as densely as possible while keeping them (bi)orthogonal, which the existence of (bi)orthogonal WH sets depends on the sampling resolution  $\mathcal{R}$ , which can be summarized as [?].

In fact, the highest bandwidth efficiency corresponds to the best use of the available dimension, which is also known as the degree of freedom of time- and band-limited signals [?], [?], [?].

Critical sampling ( $\mathcal{R} = 1$ ): Orthogonal WH sets exist. However, they have either infinite TD or FD energy spread according to the Balian-Low theory [?].

Under-critical sampling ( $\mathcal{R} < 1$ ): Neither orthogonal nor biorthogonal WH set exists.

<sup>4</sup>Suffice to say that Gabor's Gaussian pulse is probably the best candidate for the TFA domain. Also, it is known as a good example of the second generation byable communications system in global system of mobile communications (GSM) and global system of mobile communications across about 150 countries.

Therefore, we define pulse bandwidth efficiency of the transmitted signal component at the  $(m, n)$ -th TF grid point

$$Y[m, n] = \int_{-\infty}^{\infty} y(t) \gamma[t - \frac{mT}{BT_x}] e^{-j2\pi n \mathcal{F}(t-mT)} dt, \quad (23)$$

Since the functions  $g$  and  $\gamma$  in (22) are only different in terms of their TF centre, it is clear that  $\eta$  depends not only on the density of  $(g, \gamma, \mathcal{F})$  but also on the duration,  $T_g$  of  $g(t)$  and pulses occupy the whole bandwidth. Hence,

the channel equalizer is generally expensive, especially for channels exhibiting severe frequency selectivity. On the other hand, by placing the pulses as densely as possible while keeping them (bi)orthogonal, which subsequently requires a fine JTFR and a well-localized  $\mathcal{R}$ . In fact, the highest bandwidth efficiency corresponds to the best use of the available dimension, which is also known as the degree of freedom of time- and band-limited signals [?], [?].

The rationale behind the single-tap equalization of OFDM of time and band-limited signals [?], [?].

Recently, that the subcarriers in OFDM or in general MC modulations are complex sinusoids, which are the eigenfunctions of LTI systems. Their frequencies are deliberately selected to be integer multiples of the frequency resolution  $\mathcal{F}$ , which leads to the term  $n\mathcal{F}$  in (??).

Because of the discrete upper harmonic frequencies of the subcarriers, OFDM is also known as discrete multi-tone modulation, especially in the digital subscriber line technology [?].

Passing the MC signal  $x(t)$  of (??) through the LTI channel of (??), the received waveform is given by

$$y(t) = \int_{-\infty}^{\infty} x(t - \tau) h(\tau) d\tau = \sum_{n=1}^N h_n x(t - \tau_n). \quad (24)$$

Therefore, the received pulse  $y_m$  is applied to  $g(t)$  for extracting the signal component at the period  $T$  of the subcarriers, the orthogonal pulses can be obtained via truncating the subcarriers or equivalently modulating the subcarriers with the prototype pulse  $y(t) = t \Pi_{T_m}(\mathcal{T})[t, T_m, T_m + T]$ .

Clearly, the truncated subcarriers are orthogonal to each other within the symbol period  $T$  and the symbol period  $T$  of the subcarriers of a single cycle of the periodized digital symbols of  $T$ .

Considering the time dispersion of the channel, the symbol period  $T$  which is equal to the length of the bandwidth of the pulse, the extended equalization is generally performed especially for corresponding to the time dispersion of the channel and the frequency selectivity.

On the other hand, by splitting each subcarrier into two parts by the time dispersion of the channel and the frequency selectivity, the corresponding to the time dispersion of the channel and the frequency selectivity.

For example, in the case of OFDM, the subcarriers are orthogonal to each other within the symbol period  $T$  and the symbol period  $T$  of the subcarriers of a single cycle of the periodized digital symbols of  $T$ .

Therefore, the transmission of the subcarriers in OFDM is equivalent to the transmission of the subcarriers in the case of OFDM.

Therefore, the transmission of the subcarriers in OFDM is equivalent to the transmission of the subcarriers in the case of OFDM.

Therefore, the transmission of the subcarriers in OFDM is equivalent to the transmission of the subcarriers in the case of OFDM.

Therefore, the transmission of the subcarriers in OFDM is equivalent to the transmission of the subcarriers in the case of OFDM.

Therefore, the transmission of the subcarriers in OFDM is equivalent to the transmission of the subcarriers in the case of OFDM.

Therefore, the transmission of the subcarriers in OFDM is equivalent to the transmission of the subcarriers in the case of OFDM.

Therefore, the transmission of the subcarriers in OFDM is equivalent to the transmission of the subcarriers in the case of OFDM.

Therefore, the transmission of the subcarriers in OFDM is equivalent to the transmission of the subcarriers in the case of OFDM.

Therefore, the transmission of the subcarriers in OFDM is equivalent to the transmission of the subcarriers in the case of OFDM.

Therefore, the transmission of the subcarriers in OFDM is equivalent to the transmission of the subcarriers in the case of OFDM.

Therefore, the transmission of the subcarriers in OFDM is equivalent to the transmission of the subcarriers in the case of OFDM.

Therefore, the transmission of the subcarriers in OFDM is equivalent to the transmission of the subcarriers in the case of OFDM.

Therefore, the transmission of the subcarriers in OFDM is equivalent to the transmission of the subcarriers in the case of OFDM.

Therefore, the transmission of the subcarriers in OFDM is equivalent to the transmission of the subcarriers in the case of OFDM.

Therefore, the transmission of the subcarriers in OFDM is equivalent to the transmission of the subcarriers in the case of OFDM.

Therefore, the transmission of the subcarriers in OFDM is equivalent to the transmission of the subcarriers in the case of OFDM.

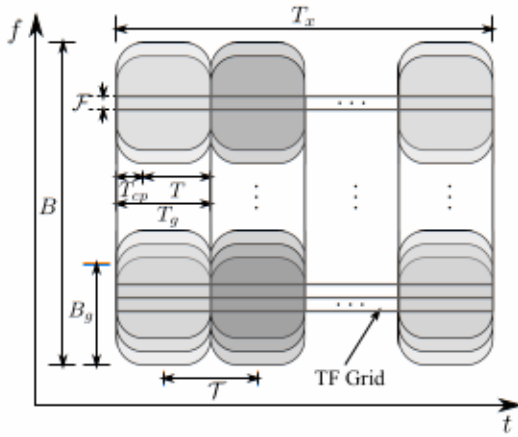


Fig. 41. TPF grid diagram showing data localization of POFDM

Considering the time dispersion of the channel and the orthogonality across a symbol period, namely the effective classification of pulses and TDM schemes.

C. Classification of Pulses and IFMC Schemes orthogonality across a symbol period, namely

Given that the pulse density obeys  $\mathcal{D} = \mathcal{R}^{-1}$ , it is clear that part of these truncated eigenfunctions. Since each MC symbol is a part of a periodic signal, the extension of the sampling of  $\mathcal{R} = 1$  achieves the highest pulse density. A plausible choice of such a  $a(t)$  is the aforementioned rectangular cyclic prefix [1], corresponding to  $y(t) = H_T(t)$  where pulse  $H_T(t)$  first proposed in [?], which corresponds to the CP-OFDM. Since its duration is constrained to the symbol period  $T_s$ , the CP-OFDM symbols are sent one after another, set [2], where  $T_B$  is usually less than  $2T_s$ . However,  $\Pi_T(t)$  theoretically has an infinite energy spread in the FD caused CP-OFDM symbol emulates an eigenfunction-based input by its slowly decaying Sinc-shaped spectrum, which agrees with the Balian-Low theory [2]. In practical OFDM systems, given the receive prototype pulse  $r(t) = \Pi_T(T_p)$ , we have  $Y[m, n] = R(nj)X[m, n]$ , which is free of ISI and are unloaded to suppress the QOBE and to ease the transmit and receive filtering [2], [?], [?]. Moreover, we may have to further broaden the signal spectrum by applying a frequency

Let a  $B_g \times T_g$  block represent the occupancy of  $g(t)$  localized TD window after cyclically extending the QFDM in the TF domain. The corresponding TF grid and the symbol by both a CP and a cyclic suffix [2], [2], [2], [2], [2] is illustrated in Fig. 11, where we obtain  $T_x = M T_g = M T$  and  $B = (N-1)T + B_g > NT$ , because  $B_g > T$ . Given a fixed  $T_x$ , the TD redundancy causes the reduction of the number of symbols and consequently erodes the bandwidth efficiency. Meanwhile, without explicitly presenting the vacant subcarriers in the FD and the cyclic extension in the bandwidth and duration of each pulse, the TF grid TD, the TLOP-based QFDM suffers from a considerable loss of bandwidth efficiency in practice due to the lack of well-localized orthogonal pulse in the case of critical sampling.

The somewhat disappointing spectral containment of the GLOP has motivated the design of a *band-limited orthogonal pulse*, that is, a pulse density job where the constraint is placed on the pulse satisfying the orthogonality condition of (1) for the periodical sampling of proximiting their theoretical limits of duration. As per this pulse is derived from the cosine function that is zero at integer intervals of the fundamental period in question, the ODF response results the GLOP of QEDM. Since its knew that a staggered frame-to-the symbol period. In BLQP, besides QEDM it is exchanged or though Dab overlapping? only the

$T_g$  is usually less than 2 TABLE. However,  $\Pi_T(t)$  theoretically has an infinite energy spread in the PD caused by its slowly decaying Sinc shaped spectrum, which agrees with the Balian-Low theory [?]. In practical Cyclic extension Scheme Pulse pulse duration, having stringent spectral restrictions, some pulse interval, some symbol interval, some subcarriers are

unloaded to suppress the OOB E and to ease the transmit and receive filtering [1]. Moreover, we may have OFDM (CP-OFDM), Ordinary rectangular pulse with vacant CP, spectrum  $T_g$  by applying a filtered OFDM to sharpen the signal edge cancellation [2]. Frequency localized TD window after cyclically extending the frequency localized TD window after cyclically extending the OFDM symbol by both a CP and a cyclic suffix [3], PS-OFDM, FBMC, T<sub>f</sub> well-localized T<sub>L</sub>OP, CP-CS, T<sub>f</sub> < T<sub>g</sub> < 2T, QAM [4], [5], [6], [7], [8], [9], [10]. Upon further taking the necessary

To take the dynamics into account, the cyclo extension of each OFDM symbol results in a lower time resolution namely an extended symbol interval of  $T > T_{SMT}^{T/2} / F$ , implying the spectrally inefficient under-critical sampling of  $R > 1$ .

As a result, by considering the vacant subcarriers in the neighboring FD subchannels are overlapped with each other FD and the cyclic extension in the TD, the TLOP-based [7]. This is in contrast to the densely overlapped subchannels of FLOP-based OFDM shown in Fig. ???. Also, in contrast to the efficiency in practice due to the lack of well-localized orthogonal pulse in the case of critical sampling, BLOP-based OFDM usually employs offset quadrature amplitude

The somewhat disappointing spectral containment of modulation signalling and is termed as OFDM/OQAM [?]. Furthermore, if we treat  $g(t)$  as the impulse response of a filter, the frequency-shifted pulses actually form a filter bank. Therefore, the OFDMA/QAM is also known as interbank multi-carrier with OQAM (FBMC/OQAM). Similarly, the TLOP-based OFDM associated with a well-localized  $g(t)$  pulse's duration  $T$  becomes much longer than the symbol interval  $T_s$ , a heavy overlap of pulses occurs in the TD. As a result, the RLOP-based QFDM is also known as staggered

With a well-localized pulse  $g(t)$ , OFDM/OQAM achieves staggered multi-tone modulation [2], [3]. In BLOP-based OFDM, in exchange for the TD overcombs, only the neighboring FD subchannels are overlapped with each other [2]. This is in contrast to the densely overlapped subchannels of TLOP-based OFDM shown in Fig. 2. Also, in contrast to valued orthogonality in (1) by real-valued orthogonality, the classic QAM signaling in TLOP-based OFDM, BLOP-based OFDM usually employs offset quadrature amplitude modulation (OQAM) signaling and is termed as OFDM/OQAM [2]. Furthermore, if we treat  $g(t)$  as the impulse response where we have  $g_{m,n} := g(t - (m\frac{T}{2})e^{j\omega_m t} + n\frac{\pi}{2})e^{jn\omega_m t}$ . In addition, due to the pulse's long duration, the channel-induced filter bank. Therefore, the OFDM/OQAM is also known ISI is usually negligible, and therefore the CP used for ISI mitigation can be omitted. As consequence, OFDM/OQAM has similarly the TLOP-based OFDM associated with a well-localized  $g(t)$  rather than with the ordinary rectangular one is called FBMC or pulse-shaped OFDM [2].

In summary, TFMC modulations designed for LTI channels adopt the eigenfunction-based transmission strategy to ease the equalization of Fig. ???. According to the different sampling, The “little magic” of the OFDM/OQAM in eigenfunction-based pulse designs, they may be categorized as the TLOP-based OFDM (OFDM or CP-OFDM, FBMC shortening the symbol interval to  $T/2$ , and at the same time replacing the complex-valued orthogonality in ?? with real-valued orthogonality), A comparison of these popular TFMC modulation schemes is shown in Table ???. Hereafter,  $\{g_{m,n}, g_{m,n}^*\}$  use the  $\{g_{m,n}, g_{m,n}^*\}_{m,n=-n}^{m,n=n}$  OFDM/OQAM, for the sake of simplicity, where we have  $g_{m,n} := g(t - m\frac{T}{2})e^{j2\pi n\mathcal{F}(t-m\frac{T}{2})}e^{j\phi_{m,n}}$ . In addition, due to the pulse’s long duration, the channel-induced ISI is usually negligible, and therefore the CP SC modulation is an impulse function based transmission used for ISI mitigation can be omitted. As consequence, OFDM/OQAM in Section ?? has the highest bandwidth efficiency and

| Comparison of Popular TFMC Modulation Schemes |   |   |           |
|---|---|---|-----------|
| Scheme  | Pulse   | Cyclic extension  | Signaling |
| OFDM (CP-OFDM)                                | Ordinary rectangular pulse with vacant edge subcarriers | $T \leq T_g < 2T$   | QAM       |
| Filtered OFDM                                 | Band allocation   | $\frac{T}{f} \leq T_g \leq 2T$  | X         |
| 4G standard [?]                               |   |   |           |
| NPS-OFDM                                      | TF well-localized FBMC                                  | CP+CS, TLOP   | QAM       |
| OFDM/QQAM                                     | TF well-localized PEBM                                  | No CP, simple QAM equalization, or the impulse function based SMT   | QAM       |
| PIFBMC/OQAM                                   | TF well-localized PEBM                                  | TF well-localized PEBM based on QAM having higher bandwidth efficiency but relatively complex channel equalization. | QAM       |

In other words, there is always a trade-off between the bandwidth efficiency and the equalization still exhibits robustness against the channel's time dispersion complexity.

In summary, TFMC modulations designed for LTI channels adopt the eigenfunction-based transmission strategy. Given  $\mathcal{F}$  and  $\mathcal{E}$ , the equalization to generate the waveform according to the MC modulation, low complexity is especially practical importance, especially when the OFDM number of subcarriers  $N$  is large. In theory, FBMC have PS-OFDM and the PEBM based OFDM (OQAM) with FBMC/QQAM (or SMT). A comparison of these popular TFMC modulations to generate  $X[m, n]e^{j2\pi n\mathcal{F}(t-mT)}$  is shown in Fig. ??, where it is noted that we will use the terms of OFDM, PS-OFDM and OQAM, for the sake of simplicity.

It is noteworthy that in contrast to the eigenfunction-based transmission of TFMC modulation, the conventional SC modulation is an impulse function based transmission, where  $g(t)$  is treated as a *transmit pulse/filter*. The other one in particular, its transmit pulses are basically the variants shown in Fig. ?? is to generate  $X[m, n]e^{j2\pi n\mathcal{F}(t-mT)}$ . Usually, they up to have  $x_m(t) = x_m(t)g(t-mT)$ , where  $g(t)$  is treated as a *prototype pulse/filter*. Once  $x_m(t), m = 0, \dots, M-1$ , these transmit pulses will lose mutual orthogonality in the presence of the channel's time dispersion, and result in a convolutional system IO relation. Meanwhile, it has been known that the SC modulation can also be combined with TD redundancy to achieve simple FD equalization and then truncate the result by the pulse  $g(t-mT)$  to obtain [?] and flexible multi-user band allocation [?]. Given its benefits, it was adopted in the 4G standard [?].

Now, one can see that for LTI channels, generally available, we can send them to a time division multiplexer we have two choices of transmission strategy: either parameterized by the symbol interval  $T$  to obtain  $x(t) = \sum_{m=0}^{N/2-1} x_m(t)$ , as in (??). It is noteworthy that the filter bank function based one having higher bandwidth efficiency and the pulse-shaping seen in Fig. ?? exactly tally the terminology of FBMC and PS-OFDM, respectively, but relatively complex channel equalization. In other

However, these two methods require  $N$  modulators, and words, there is always a trade-off between the bandwidth therefore have prohibitively high implementation complexity.

The implementation of MC modulation was considered unreasonable, until the connection between the inverse discrete Fourier transform and the Fourier transform, and the MC modulation demodulation was found in [?], where an analog hardware based implementation of the IDFT was employed

Given  $\mathcal{F}$ ,  $\mathcal{E}$  and  $g(t)$ , how to generate the waveform hardware based implementation of the IDFT was employed to generate the MC waveform. After that, the inverse fast Fourier transform and fast Fourier transform algorithms [?] were introduced in [?] to realize the IDFT and DFT which leads to the widely adopted IFFT/FFT-based implementation of MC modulation in Section ??.

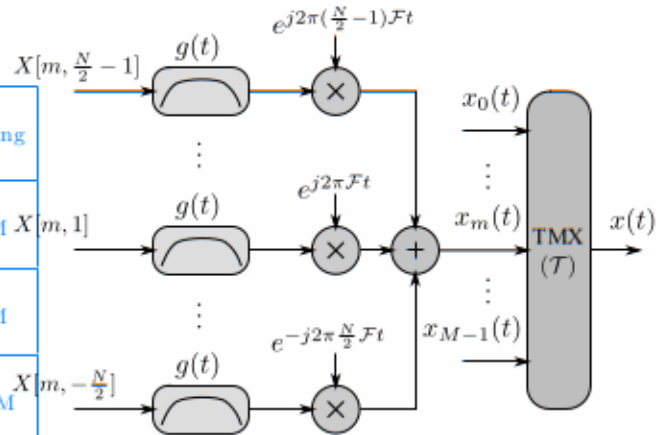


Fig. 5. Analog implementation with  $g(t)$  as transmit pulse/filter

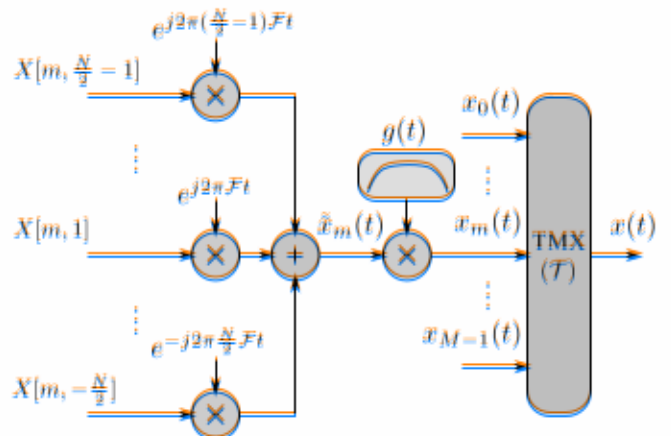


Fig. 6. Analog implementation with  $g(t)$  as prototype pulse/filter function

As shown in Fig. ??, the generation of  $x(t)$  or  $x_m(t)$  using carrier frequencies of  $n\mathcal{F}$  depends on the digital implementation of  $X[m, n]e^{j2\pi n\mathcal{F}t}$ . As shown in Fig. ??, one approach of them [?] to generate  $X[m, n]e^{j2\pi n\mathcal{F}t}$  is to modulate it according to  $j2\pi n\mathcal{F}(t-mT)$ , and then add them up. The first observation is that although  $x_m(t)$  has to obtain bandwidth of  $B > N\mathcal{F}$ ,  $\tilde{x}_m(t)$  in (??) is strictly band-limited to  $[-\frac{N}{2}\mathcal{F}, (\frac{N}{2}-1)\mathcal{F}]$ . Because the highest frequency is  $\frac{N}{2}\mathcal{F}$ , sampling  $\tilde{x}_m(t)$  at the Nyquist rate of  $N\mathcal{F} = N/T$  becomes feasible by obeying the sampling theorem. Then, the  $N$  samples of  $\tilde{x}_m(t)$  within one period  $T = \frac{1}{\mathcal{F}}$  are given by where  $g(t)$  is treated as a transmit pulse/filter. The other one shown in Fig. ?? is to generate  $X[m, n]e^{j2\pi n\mathcal{F}(t-mT)}$  add  $\tilde{x}_m(t) \triangleq \tilde{x}_m(t + \frac{n}{N}) = \sum_{n=-N/2}^{N/2-1} X[m, n]e^{j2\pi \frac{n}{N}\mathcal{F}t}$  (29)

for  $0 \leq n \leq N-1$ , which exactly represent the IDFT of  $[X[m, 0], \dots, X[m, \frac{N}{2}-1], X[m, -\frac{N}{2}], \dots, X[m, -1]]^T$ . The second observation is that  $\tilde{x}_m(t)$  is an infinite-length periodic signal, which results in that pulse  $g(t)$  repeat to sample  $x_m(t)$  in one period  $T$  to obtain where samples is treated as a prototype pulse, or window function. Once  $x_m(t)$  can be generated by passing a filterable window function  $\frac{T}{N}$  time division  $\frac{T}{N}$  multiplication through a windowed IDFT with the passband bandwidth  $B$  to [?] at which  $t_i$  is actually the interpolation (??) of  $t$ . It is the digital to that the filter bank having Bigate band. After that, the going based windowing is applied to the windowing (of FBMC and PS-OFDM, respectively)  $B = (N-1)\mathcal{F} + B_g >$

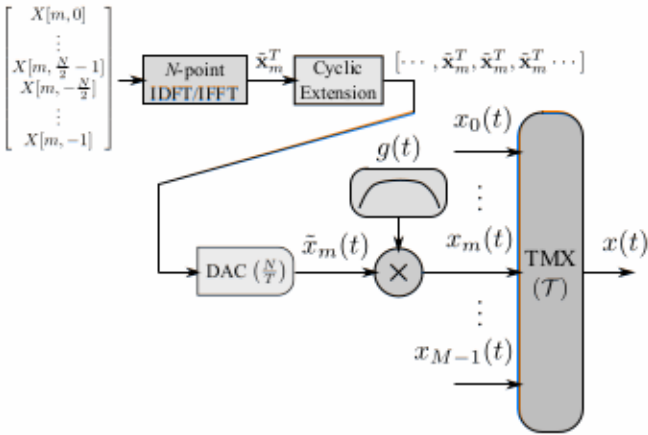
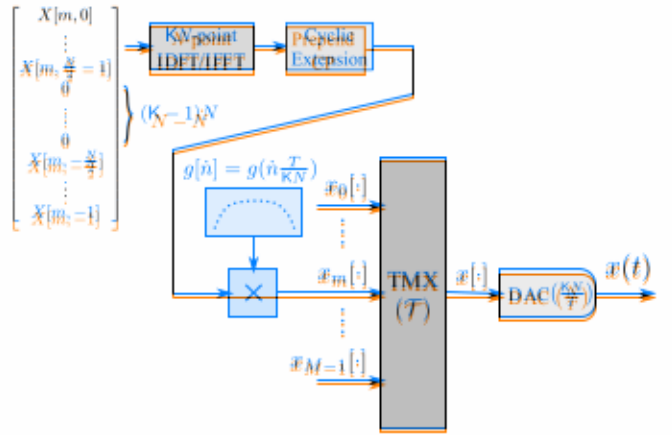


Fig. 7.11 Digital implementation with  $h(t) = g(t)$  as input plus previous window function



**Fig. 9. Vacuum edge subcarriers based digital implementation (Filtered OFDM)**

However, these two methods require  $N$  modulators, and therefore have prohibitively high implementation complexity. The implementation of MC modulation was considered unreasonable, until the connection between the inverse discrete Fourier transform, the discrete Fourier transform, and the MC modulation/demodulation was found in [?], where an analog hardware based implementation of the IDFT was employed to generate the MC waveform. After that, the inverse fast Fourier transform and fast Fourier transform algorithms [?] were introduced in [?] to realize the IDFT and DFT, which leads to the widely adopted IFFT/FFT-based implementation of MC modulation [?].

As shown in Fig. ??, the generation of  $x(t)$  or  $x_m(t)$  using the IFFT relies on a digital implementation of the second analog approach of Fig. ??, which is based on the following two observations. The first observation is that  $NF$  when  $B_{\text{eff}} > F$ . It should be noted that the windowing although  $x_m(t)$  has a bandwidth of  $B > NF$ ,  $x_m(t)$  in (??) and time multiplexing can also be conducted in the digital is strictly band-limited to  $[-\frac{N}{2}F, (\frac{N}{2}-1)F]$ . Because the domain before the DAC if their implementation is performed highest frequency is  $\frac{N}{2}F$  sampling  $x_m(t)$  at the Nyquist at an oversampling rate of  $K$  where  $K > 1$  is an integer rate of  $NF = N/T$  becomes feasible, by obeying the representing the oversampling factor. The oversampling based sampling theorem. Then, the  $N$  samples of  $x_m(t)$  within implementation of MC modulation is shown in Fig. ??.

In practice, given the appropriate parameter settings, the cyclic extension of  $\tilde{\mathbf{x}}_m^T$  and the subsequent windowing can be omitted for further simplifying the implementation. Recall that  $E_m(t) = \mathbf{f}_m^H(\mathbf{h}(t))$  and  $\sum_{n=1}^N X[m, n]e^{-j\frac{2\pi}{N}nt} = 0$  for the IFFT. Then  $x_m(t)$  becomes approximately band-limited to  $-\frac{N}{2}F \leq f \leq \frac{N}{2}F$ , which exactly represent the IDFT of  $X[m, 0:N]$ . In fact, a practical OFDM system often only has  $N < N$  subcarriers, resulting in  $\tilde{x}_m(t)$  is an infinite-length periodic signal, which indicates that we can repeat  $N$  samples in one period to obtain the samples of  $\tilde{x}_m(t)$ . Let  $\tilde{\mathbf{x}}_m(t) \triangleq [\tilde{x}_m[0], \dots, \tilde{x}_m[N-1]]e^{j2\pi n F(t-nT)}$ . Then  $\tilde{x}_m(t)$  can be generated by passing the cyclic extension of  $\tilde{\mathbf{x}}_m^T$  namely  $[\dots, \tilde{\mathbf{x}}_m^T, \tilde{\mathbf{x}}_m^T, \tilde{\mathbf{x}}_m^T \dots]$  through an ideal LPF with passband  $\frac{N}{2}F$  and stopband  $\frac{N}{2}F$ . The subcarriers are usually intentionally filtered in this RRC-like design of filter. With  $N$  vacant subcarriers, After the band-selective windowing  $\mathbf{B}_m$  is applied to  $\tilde{\mathbf{x}}_m(NF)$ , where the setting of  $\mathbf{B}_m$  bandwidth corresponds to the  $B_m$  (Nyquist) overampling factor  $M$ . As the implementation of the channel block, we can apply a window function  $w_m(t)$  to the channel

also be conducted in the digital LPF domain before the DAC, if their implementation is impractical, implying that the simple truncating ratio of  $K_m^N$ , where  $K_m$  is already integer implemented, is vacated by subcarriers based on Fig. ?? The method, which has been implemented in practice because of its bandwidth flexibility, is shown in Fig. ?? Given the appropriate parameter settings, the cyclic extension of  $x_m^T$  sample-wise pulse shaping windowing can be omitted for filtered OFDM [1], where the implementation rate among subcarriers will be crossed, especially for those usually band edge. This problem can be avoided by becoming approximately blank limited to a result, filtered OFDM can be considered as OFDM subcarriers with a bending edge pulse and preselected QPSK systems, as shown in Table ??  $N - \bar{N}$  subcarriers, resulting in noteworthy that since the interpolation filter in a DAC is exactly an LPF, practical OFDM systems with the vacant subcarriers based implementation are actually filtered OFDM systems. The simulations of such OFDM systems are usually performed based on TD samples with  $\frac{1}{NF}$ -interval, where the direct current subcarrier is also usually left unmodulated to ease the RF circuit design [1]. With  $N - \bar{N}$  In comparison to the convenient IFFT-based implementation of the OFDM and PS-OFDM, the implementation of OFDM/OQAM has a considerably higher complexity owing to the overlapping of MC symbols shaped by the long-duration based implementation of Fig. ?? Then, we can pass  $x_m^T(t)$ . An elegant approach to alleviate this difficulty is to amalgamate the IFFT with a polyphase network for efficiently realizing a filter bank [31, 32]. This approach is essentially for ED equivalent of the aforementioned TD operations, including the cyclic extension and the windowing/pulse shaping.

Förlängt lyrselquitivdelelfly schapelwisen forse att hängit ifr  
 6FDM InPF OFDM/QQAMeped oFDM till [?]. However when the  
 orthogonality is denegd synchrotrons will be emded to spefically  
 have chosen devite band studying TGOFDM. Re transmisson with  
 by ushly siege edge channels. Basell un [different] appntx filtered  
 OFDM TV-GIR band thsi desadants no OFDmais socibanded wFD  
 channeg in atr pulsee and Vahame ledges in subcarriare, qualisation  
 ineffimite? can be found in [?], [?], [?], [?], [?], [?], [?], [?], [?],  
 [?]. It [?] als [?] no [?] ward the refimmed the interpolation pntimed  
 ou DACT is the off diagonal LP elements of the QFEDM system with

However, these complex TV-CIR channel models often suffer from expensive yet somewhat inaccurate channel estimation. This is because the TV-CIR has a large number of parameters even along<sup>0</sup> with a low-rank approximation. For OFDM/OQAM, due to its intrinsic imaginary interference caused by the real-valued orthogonality constraint, the channel-induced ISI and ICI remain cumbersome. To the best of our knowledge, there is no potent equalization solution for OFDM/OQAM operating in high-mobility environments, where single-tap equalizers fail to achieve satisfactory performance [?].

On the other hand, in the spirit of eigenfunction-based transmission, PS-OFDM schemes for achieving a scalar IO relation for transmission over LTV channels can be found in [3], [7], [2], [2] and the references therein. It is widely known [Fig. 9] that the underspread LTV channels at best have a structured set of approximate eigenfunctions [?]. Owing to the necessity to consider both time and frequency dispersions, these approximate eigenfunctions may only hold actually in the channel's spreading or scattering functions, but also require a well localized prototype pulse  $g(t)$  and a much coarser IFFT interval  $\Delta f$ , which is appropriate, then corresponding pulses can be considered as an approximation of the orthogonal WHT sets in the case of under-critical sampling of  $R > 1$ , and therefore require no idle subcarriers. In comparison to the conventional IFFT-based implementation of the OFDM and PS-OFDM, the implementation of residual IQQAM has considerably higher complexity owing to the overlapping of MC symbols shaped by the long channel  $g(t)$ . Realizing eigenfunction-based transmissions in LTV channels is amalgamated with the IFFT with a polyphase network for efficiently realizing a filter bank [?], [2]. This approach is the second one to the conceptually reduced bandwidth dependency associated with the cyclic extension (CRE) in summing/pulse shaping. TFMC modulations designed for eigenfunction-based transmissions in LTI channels suffer not only from costly and inaccurate channel estimation, but also from complex equalization in LTV channels. On the other hand, for PS-OFDM designs, LTV eigenfunction-based transmission in OFDM than OFDM/IQQAM performs well. However, exhibiting bandwidth efficiency in practice, numerous efforts have been devoted to studying OFDM for transmission over doubly-selective channels. Based on

different approximations of the TV-CIB and the resultant

The challenges imposed by eigenfunction-based transmission in ETV channels motivate us to consider new transmission strategies and develop alternative modulation schemes. To this end, it is necessary to reconsider the properties of LTV and the references therein. It was pointed out that the channels and design specifically tailored channel-oriented pulses offer time diversity or Doppler diversity [?, ?]. However, these complex TV-CIR channel models often suffer from expensive yet somewhat inaccurate channel estimation. This mismatch between transmitter and receiver pulses and parallel frequency bands along with a lossy channel should be accounted for OFDM/OQAM and its intrinsic self-interference cancellation. The eigenfunctions of ISIT and IIG represent two basic but potentially best common properties for LIE. The DDF potential equalization solution proposed for OFDM/OQAM operating in high-mobility

Recall that, due to single-limited bandwidth failure, the transmission of a signal is performed by serving an ESDD channel at the receiver. The ESDD channels inherit the eigenfunction-based signal transmission (PS-QFDM), which is fully covering all the IOM-related properties of the ESDD channel. It is known that those of DD channels. [As shown in (3) and the references therein, if ESDD channels are discretized with a spectral TV solution, without the Doppler resolution set, the corresponding eigenfunctions are orthogonal. Owing to the unitarity property, consider a result in which the frequency diversity of the channels approximate eigenfunctions, they corresponding to the DD channel, help dealing with ISI and fading. Double burst solutions, which are de-correlated through the signal of bandwidth, are coarser JTFR than that of OFDM [7]. Since in fading, the Doppler fading pulses have the same bandwidth as the time and frequency responses (by orthogonal sidelobes), the JTFR is the same as the DD domain with a slight loss of resolution and therefore the quality of the TDD link. To address design difficulties, spreading phase approximation nature of these eigenfunctions leads to residual ISI and ICI, which may still remain cumbersome. But DD can be 2D impulse response. As a result, there are two main challenges in realizing eigenfunction-based transmission in LTV channels. The first one is the adoption of the ESDD channel's 2D impulse response, which is *literally* time-invariant. Recall that the gridded DD domain has the physical units of time and frequency, so it is also a gridded TF domain, but the DD domain is able to resolve delay and coarse JTFR with much finer resolution. As we will show below, In summary, the conventional TECM modulations designed for eigenfunction-based transmissions in LTV channels is exactly due to the mismatch between the modulation and the channel. Let us consider passing an MC signal  $x(t)$  through the channels. On the other hand, PS-QFDM, designed for eigenfunction-based transmission in LTV channels have severe practical challenges and exhibit low bandwidth efficiency.

$$y(t) = \sum_{p=1}^P h_p x(t - \tau_p) e^{j2\pi f_p(t - \tau_p)}, \quad (31)$$

$$= \sum_{p=1}^n n_p x(t - \tau_p) e^{s(t-\tau_p)}, \quad (31)$$

where  $x(t)$ , in (2), can be rewritten as  $x(t) = \sum_{m=0}^{M-1} x_m(t)$ . Assume that we set a large enough  $T \geq T_0 + \tau_{\text{max}}$  for completely isolating MC symbols from each other and preventing ISI. Then, from (2), the  $m$ th received MC symbol is given by

$$x_m(t) = \sum_{p=1}^P h_p \sum_{n=0}^N Y_n(t - mT - \tau_p)$$

$$\cdots e^{j2\pi n F_c(t - mT - \tau_p)} e^{j2\pi \nu_p(t - \tau_p)}$$

## A. Common Properties of ESDD Channels

In practical transceivers, the transmit and receive pulses are usually fixed. Therefore, these pulses should be designed according to the common properties of LTV channels. However, in contrast to LTI channels relying on the complex sinusoidal envelope, has Doppler-induced properties dispersion, basically known as the property for LTV or DD channels, due to the frequency propagation environments of OFDM systems. Since usually  $\nu_p/F \notin \mathbb{Z}$ , this kind of fractional CFO will limited bandwidth and duration of the signal implicitly observe in ESDD channel at the receiver. Thus the ESDD channel is the one that matters for signal transmissions. Then what we really care about is the common properties of ESDD channels,

rather than those of (DD). In fact, as we have shown in (??), the corresponding functions of (ESDD) holds regardless of whether the channel is flat or not. This shows that the ISI and ICI are the same for both DD and ESDD channels. As a result, although the channel is flat, the corresponding ISI and ICI are the same for both DD and ESDD channels.

## B. DD Domain 2D Impulse Response

The discretized spreading function  $\text{ESDD Channel}(?)$  can be viewed as the ESDD channel's 2D impulse response, which is literally time-invariant. Bearing in mind that  $\tau_p = l_p/W$ ,  $\nu_p = k_p/T$ , and  $l_p, k_p \in \mathbb{Z}$ , one can see from (??) that if  $\mathcal{F} = 1/T$ , we have  $\nu_p/T = k_p \in \mathbb{Z}$ , and then the ICI becomes aligned with the frequency resolution  $1/T$ , which has a similar effect to delay and Doppler with much finer resolution. As we will show below, the complex ICI of OFDM or OFDM/QAM is  $1/T$ . In other words, if we can design a DDMC in LTV channels is exactly due to the mismatch between modulation and the channel.

Let us consider passing an MC signal  $x(t)$  through the ESDD channel of (??). The received waveform is given by

$$x(t) = \sum_{m=0}^{M-1} \sum_{n=-N/2}^{N/2-1} X[m, n] g\left(t - \frac{n}{W}\right) e^{j2\pi\nu_p(t-\tau_p)}, \quad (34)$$

$$y(t) = \sum_{p=1}^P h_p x(t - \tau_p) e^{j2\pi\nu_p(t-\tau_p)}, \quad (35)$$

the time and frequency resolutions of which are identical to those of the ESDD channel, the ISI and ICI will be aligned to where  $x(t)$  in (??) can be rewritten as  $x(t) = \sum_{m=0}^P x_m(t)$ . Assume that we set a large enough  $P \geq T_g + \tau_{\max}$  for  $x_m(t)$  is only interfered by a minimum number of its neighbor symbols, and the pattern of the whole interference become compact. Further considering that the delay resolution  $1/W$  and the Doppler resolution  $1/T$  are common properties of ESDD channels, the DDMC modulation in (??) seems to be an appropriate modulation scheme for the ESDD channels.

The aligned ISI and ICI can also be interpreted using the relation between the STFT of  $x(t)$  and  $y(t)$  in (??). Note that the STFT is equivalent to applying receive pulses (analysis window) to extract the signal components in the MC modulation. Similar to (??), upon substituting  $S(\tau, \nu) = h(\tau, \nu)$  and  $t = m/W$ ,  $f = e^{j2\pi\nu_p(mT_g - \tau_p)}$  into (??) to extract the signal component at the  $(m, n)$ -th TF grid point, we have

$$Y[m, n] = Y^{(g)}\left(\frac{m}{W}, \frac{n}{T}\right) e^{j2\pi\nu_p(mT_g - \tau_p)}, \quad (36)$$

Eq. (??) also implies that for  $x_m(t)$ , the ESDD channel is

$$\propto e^{-j2\pi\frac{\tau_p(n-k_p)}{W}}. \quad (37)$$

Then, we have the following proposition.

**Proposition 1.** (*If*) If the transmitted impulse response  $g(t)$  holds regardless of  $W$  and  $T$ , and

the ISI exists for the ESDD channel of OFDM, the phase component of the  $(m, n)$ -th signal coefficients is the phase difference between common phase errors of two adjacent OFDM symbols corrupted by the same CFO  $k_p$  [?]. As a result, for a signal consisting of time-multiplexed symbols, different symbols experience different ESDD channels, where these ESDD channels have the same number of paths. By substituting the orthogonality property of (??), (??) can be obtained straightforwardly. Proposition 2D reveals the position of an ESDD channel for DDMC over ESDD channels. The proof is similar to that of integer CFO [?]. Similar results can also be obtained straightforwardly for the DD channel. In (??), the DDMC can be described as a 2D convolution between the transmitted digital symbols and the ESDD channel. Upon considering the impulse function  $g(t)$ , transmission strategy of ESDD channel, the resultant 1D convolutional IO relation over LTI channels, it becomes clear that the DDMC modulation is an impulse function based transmission for ESDD channels. Apparently, an appropriately designed  $g(t)$  is necessary to realize such an impulse function-based transmission. However, to that of integer CFO [?], the same thing happens to the ISI if  $T_g = 1/W$ . In other words, if we can design a  $1/(4\pi)$ , which violates the Heisenberg uncertainty principle. Therefore, DDMC does not exist [?]. Meanwhile, because the JTFR is now  $R_{\text{DDC}} = 1/(\text{WT}) \ll 1$ , according to the WH frame theory,  $(W)$  orthogonal WH sets do not exist [?]. Hence, it seems impossible to perform DD domain modulation, due to the lack of pulses. In the following sections, we will discuss progress in the design of DD domain modulation to those of the ESDD channel, the ISI and ICI will be *Digital OTFS Modulation* over ESDD channel grid. As a result, each transmitted symbol is only interfered by the DD domain was first considered in form of the OTFS modulation, whose interference phenomena is compact. Further considering the modulation resolution  $1/W$  and the DD domain to the TF domain by the ISFFT precoder. Then, it modulates the duration in (??) using the suitable CP mechanism, and prepends the ESDD based CP for the whole OTFS frame.

The aligned ISI and ICI can also be interpreted using the relation between the STFT of  $x(t)$  and  $y(t)$  in (??). Note that the STFT is equivalent to applying receive pulses (analysis window) to extract the signal components in the MC modulation. Similar to (??), upon substituting  $S(\tau, \nu) = h(\tau, \nu)$  and  $t = m/W$ ,  $f = e^{j2\pi\nu_p(mT_g - \tau_p)}$  into (??) to extract the signal component at the  $(m, n)$ -th TF grid point, we have

$$\hat{x}(t) = \sum_{\hat{n}=0}^{N-1} \sum_{\hat{m}=0}^{M-1} X[\hat{n}, \hat{m}] g(t - \hat{n}T_0) e^{j2\pi\hat{m}F_0(t - \hat{n}T_0)},$$

$$Y[m, n] = Y^{(g)}\left(\frac{m}{W}, \frac{n}{T}\right) \quad (37)$$

where  $X[\hat{n}, \hat{m}]$  is obtained by the ISFFT of  $\hat{x}(t)$  as  $\hat{n} = \frac{l_p}{W}, \hat{m} = \frac{n - k_p}{T}$

$$X[\hat{n}, \hat{m}] = \frac{1}{\sqrt{MN}} \sum_{m=0}^{M-1} \sum_{n=0}^{N-1} X[m, n] e^{j2\pi\left(\frac{\hat{n}}{N} - \frac{\hat{m}}{M}\right)}. \quad (38)$$

Note that in OTFS,  $M$  and  $N$  are also the number of subcarriers and symbols of the underlying OFDM modulation respectively. If we transmit  $p$  sets of  $(t)$  OTFS waveform designed in the typical  $R_0 = \text{TF}$  delay  $\tau = 1/W T_0$  and

The ideal resolution of OTFS in ESDD is similar to the received signal group over time at the receiver [2]. Roughly speaking, this means that the pulses  $g(t - \hat{n}T_0)e^{j2\pi m F_0(t - \hat{n}T_0)}$  for different  $m$  or  $n$  in (??) are (bi)orthogonal with each other, even after experiencing the time and frequency dispersion induced by the channel. Given this ideal pulse, OTFS expects to achieve a 2D convolution between the transmit symbols  $X[m, n]$  (36) and the channel  $h(\tau, \nu)$  at the channel output [?]. Unfortunately,

**Proof.** By substituting the orthogonality property of the assumed ideal pulse cannot be realized in practice [?], (alt) into (??), (??) can be obtained straightforwardly. ■

The underlying reason may be that the pulses satisfying the Proposition ?? reveals the basic form of the IO relation biorthogonal robustness property essentially correspond to DDMC over ESDD channels. From (??) one can see the eigenfunction-based transmission that achieves a scalar that except for some phase terms, the extracted signal IO relation over the LTV channel, which requires  $\mathcal{R} \geq 1$ , component at each TF grid point in the DDMC can be as mentioned in Section ?? Since the OTFS waveform is described as a 2D convolution between the transmitted designed for  $\mathcal{R} = 1$ , the corresponding TLOP cannot be digital symbols and the ESDD channel. Upon considering biorthogonal robust.

Due to the lack of ideal pulse, the rectangular pulse  $\Pi_{T_0}(t)$  modulation and the resultant 1D convolutional IO relation has been widely adopted in current OTFS studies [?], which over LTI channels, it becomes clear that the DDMC is the TLOP for the CP-free OFDM with  $\mathcal{R} = 1$ . Recall modulation is an impulse function based transmission for that for the CP-free OFDM, some vacant edge subcarriers are ESDD channels. necessary to suppress the OOB, as mentioned in Section ?? Apparently, an appropriately designed  $g(t)$  is necessary ?? Since OTFS relies on CP-free OFDM, OOB is also to realize such an impulse function based transmission, an inevitable practical issue for OTFS [?]. However, letting However, the impulse in the DD domain or DDLP has  $X[n, m] = 0$  for a part of  $\hat{m}, 0 \leq \hat{m} \leq M - 1$  may break the a TFA less than  $1/(4\pi)$ , which violates the Heisenberg inherent connection between  $X[n, m]$  and  $X[\hat{n}, \hat{m}]$  governed uncertainty principle. Therefore, DDLP does not exist by the ISFFT precoder in (??), as  $X[n, m]$  is drawn from Meanwhile, because the JTFR is now  $\mathcal{R}_{DD} = 1/W_1 < 1$  a QAM constellation. Also, the absence of CP and CS in according to the WH frame theory, (bi)orthogonal WH CP-free OFDM makes the windowing-based OOB mitigation sets do not exist either. Hence, it seems impossible to methods infeasible, while letting  $g(t)$  in (??) be a spectrally compact pulse leads to severe performance degradation [?]. In the following sections, we will discuss progress in the due to loss of orthogonality. Furthermore, it is noteworthy that design of DD domain modulation. from (??), the expected 2D convolution may be unachievable, considering the phase terms induced by the time-varying path Due to the lack of ideal pulse, the rectangular pulse  $\Pi_{T_0}(t)$  in (??) is necessary ?? Since OTFS relies on CP-free OFDM, OOB is also an inevitable practical issue for OTFS [?]. However, letting  $X[\hat{n}, \hat{m}] = 0$  for a part of  $\hat{m}, 0 \leq \hat{m} \leq M - 1$  may break the inherent connection between  $X[n, m]$  and  $X[\hat{n}, \hat{m}]$  governed by the ISFFT precoder in (??), as  $X[n, m]$  is drawn from a QAM constellation. Also, the absence of CP and CS in CP-free OFDM makes the windowing-based OOB mitigation methods infeasible, while letting  $g(t)$  in (??) be a spectrally compact pulse leads to severe performance degradation [?].

**E. DDMC/DDM Modulation** Motivated by OTFS's concepts of modulating information bearing symbols in the DD domain and DD grid, we present challenges, the OTFS modulation transforms the signals from the DD domain to the TF domain by the ISFFT precoder. Then it modulates the transformed signals using the  $\mathbb{F} = \frac{N}{M}$  into (??) for the sake of comparison. Then, the symbol-wise CP-free OFDM, and prepends a frame DDMC modulation waveform becomes based CP for the whole OTFS frame.

Let  $\mathcal{H} = \frac{N/2-1}{M}$  and  $T_0 = 1/F_0$ . Then the TF domain grid of OTFS obeys  $X[nT_0, mT_0]$  for  $n = \frac{T_0}{M}, \dots, N-1$  and  $\hat{m} = 0, \dots, M-1$  while the corresponding DD domain grid is defined as  $\left\{ m \frac{T_0}{M}, n \frac{1}{NT_0} \right\}$  for  $m = 0, \dots, M-1$  and where the time and frequency resolutions of an OTFS frame without the frame-wise CP can be written as [?] Differences between the OTFS waveform in (??) and the DDMC waveform in (??) are the resolutions in the time (delay) domain ( $T_0$ ) in time v.s.  $\frac{1}{M}T_0$  in delay) and the frequency (Doppler) domain ( $\frac{1}{T_0}$  in frequency v.s.  $\frac{1}{NT_0}$  in Doppler). (37)

Now the crucial question is whether there exists a DDOP denoted  $\mathcal{A}[n, m]$  is obtained by the ISFFT respect to both the time (delay) resolution  $\mathcal{T} = \frac{T_0}{M}$  and the frequency (Doppler) resolution  $\mathcal{F} = \frac{1}{NT_0}$ . If such a DDOP does exist, we can realize this hypothetical DDMC modulation by letting  $g(t) =$

Note that in OTFS,  $M$  and  $N$  are also the number of subcarriers and symbols of the underlying OFDM modulation, respectively. Observe from (??), the OTFS waveform is designed exactly with  $\mathcal{R} = \mathcal{T}\mathcal{F} = 1$ , because  $\mathcal{T} = \mathcal{F} = T_0$ .

The ideal pulse of OTFS in (??) is said to satisfy the biorthogonal robustness property [2]. Roughly speaking, this means that the pulses  $g(t - \hat{n}T_0)e^{j2\pi m F_0(t - \hat{n}T_0)}$  for different  $m$  or  $n$  in (??) are (bi)orthogonal with each other, even if experiencing  $g(t)$  is much a DDOP due to dispersion induced by the channel given this ideal pulse, OTFS expects to achieve a 2D convolution between the transmit symbols  $X[m, n]$  and the channel  $h(\tau, \nu)$  at the channel output [?]. Unfortunately, the assumed ideal pulse cannot be realized in practice [?]. The underlying reason may be that the subpulse  $g(t)$  is a square-root Nyquist pulse property, as it is zero ISI interval  $T_0/M$  and its duration  $T_0 = 2Q\frac{T_0}{M}$ , where  $Q$  is a positive integer. Figure ?? illustrates the unique structure of the DDOP  $g(t)$  in Section ?? Since the OTFS waveform is designed for that  $u(t)$  satisfies the orthogonal TLOP property of biorthogonal robust.

Due to the lack of ideal pulse, the rectangular pulse  $\Pi_{T_0}(t)$  has been widely adopted in current OTFS studies [?], which is the TLOP for the CP-free OFDM with Ambiguity. Recall that for  $g(t)$  defined as the CP-free OFDM, some vacant edge subcarriers are necessary to suppress the OOB, as mentioned in Section ?? Since OTFS relies on CP-free OFDM, OOB is also an inevitable practical issue for OTFS [?]. However, letting  $X[\hat{n}, \hat{m}] = 0$  for a part of  $\hat{m}, 0 \leq \hat{m} \leq M - 1$  may break the inherent connection In other words,  $u(t)$  is orthogonal with respect to the delay between  $X[n, m]$  and  $X[\hat{n}, \hat{m}]$  governed by the ISFFT and Doppler resolutions of the ESDD is channel within the range of interest  $|\hat{m}| \leq M - 1$  and  $|\hat{n}| \leq N - 1$ . After prepending constellation. Also, the absence of CP and CS in CP-free OFDM makes the windowing-based OOB mitigation frame is sent through the channel.

Let us assume that the maximum delay and Doppler of the compact pulse leads to severe performance degradation [?]. ESDD channel in (??) are  $(L-1)\frac{1}{M}$  and  $K\frac{1}{N}$ , respectively due to loss of orthogonality. Furthermore, it is noteworthy that from (??), the expected 2D convolution may be channel-achievable, considering the phase terms induced by the time-varying path gains.

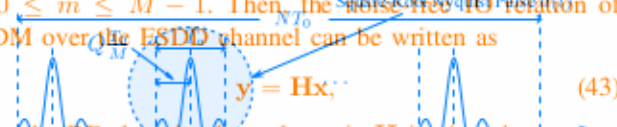
**DDMC/DDM Modulation** Motivated by OTFS's concepts of modulating information bearing symbols in the DD domain and DD grid, we present challenges, the OTFS modulation based on  $u(t)$  in DD grid, we present a general DDMC signal design in this section. Considering the DD domain grid in OTFS, signal component at the  $(n, m)$  th TF grid point, namely, for the  $n$  th subcarrier of the  $m$  th DDMC symbol. Let us change  $V[n, m]$  and  $X[m, n]$  in two vectors as

$$x(t) = \sum_{m=0}^{M-1} \sum_{n=-N/2}^{N/2-1} V[n, m] u(t - nT_0) e^{j2\pi n \frac{1}{NT_0} (t - m\frac{T_0}{M})}, \quad (39)$$

where

where the time and frequency resolutions are  $\mathcal{T} = \frac{T_0}{M} = \frac{1}{MF_0}$  and  $\mathcal{F} = \frac{1}{NT_0} = \frac{1}{N} = \frac{1}{NF_0}$ , respectively. The main differences between the OTFS waveform in (??) and the

for  $0 \leq m \leq M - 1$ . Then, the noise-free IQ relation of ODDM over the ESDD channel can be written as



where the DD domain channel matrix  $\mathbf{H}$  is given by

$$\mathbf{H}_0^0 \quad \mathbf{H}_{L-1}^0 \mathbf{D} \quad \dots \quad \dots \quad \mathbf{H}_0^0 \mathbf{D}$$

Fig. 10. Delay Doppler domain orthogonal pulse (DDOP)  $u(t)$ .

DDMC waveform in (??) are the resolutions in the time (delay) domain ( $T_0$  in time v.s.  $\frac{T_0}{M}$  in delay) and the frequency (Doppler) domain ( $\frac{1}{NT_0}$  in frequency v.s.  $\frac{1}{NT_0}$  in Doppler):

Now the crucial question is whether there exists a DDOP denoted by  $u(t)$ , that is orthogonal with respect to both the time (delay) resolution  $\mathcal{T} = \frac{T_0}{M}$  and the frequency (Doppler) resolution  $\mathcal{F} = \frac{1}{NT_0}$ . If such a DDOP does exist, we can realize this hypothetical ODDM modulation by letting  $g(t) = u(t)$  in (??). According to [?], such a DDOP with

$$\mathbf{H}_l^m = \sum_{k=0}^K \theta(\hat{n}+1, K+1, l) e^{j2\pi \frac{\hat{k}(m-1)}{MN}} \mathbf{C}^{\hat{k}}, \quad (45)$$

$$a(t) = \sum_{k=0}^K a(t - \hat{n}T_0), \quad (40)$$

$$\mathbf{D} = \text{diag}\left\{1, e^{-j\frac{2\pi}{N}}, \dots, e^{-j\frac{2\pi(N-1)}{N}}\right\}, \quad (46)$$

where the subpulse  $a(t)$  is a square-root Nyquist pulse parameterized by its permutation intervals  $T_0/M$  and its duration  $T_a = 2Q\frac{T_0}{M}$ , where  $Q$  is a positive integer.

Figure ?? illustrates the unique structure of the DDOP  $u(t)$ . When  $2Q \ll M$  and therefore  $T_a \ll T_0$ , it has been proved that  $u(t)$  satisfies the orthogonality property of

$$\mathcal{A}_{u,u} \left( \frac{T_0}{M}, n, \frac{1}{NT_0} \right) = \delta(m)\delta(n), \quad (41)$$

As an  $MN \times MN$  block-circulant-like matrix, the DD domain channel matrix  $\mathbf{H}$  in (??) represents the linear combination between  $X[m, n]$  and the ESDD channel  $h(\tau, \nu)$ . Upon using the DDOP  $u(t)$  of Fig. ?? as the transmit and receive prototype pulses,  $\mathcal{A}_{u,u}(\tau, \nu)$  becomes capable of outperforming the OTFS in terms of both its OOBE and bit error rate [?], [?]. It is noteworthy that with the DDOP (namely the pulse-chain  $u(t)$ ), the ODDM can be viewed as a PS-OFDM or more precisely Inphase and quadrature-shaped OFDM orthogonal with respect to the delay and Doppler lobes of its DDOP ESDD channel within the range of interest because of the conventional understanding after preorthogonal pulse synthesis for the bandwidth WH is in (??) due to the ODDM frame itself through the channel  $1/(NT_0) = 1/MN$ . Let us assume that the maximum delay and Doppler of the ESDD channel are  $(M-1)$  and  $(N-1)$ , respectively. Then the fundamental (bi)orthogonal pulse design principle previously defined in the previous section in which  $(2K+1)$  be DD domain channel matrix  $\Theta$ , where each row and each column of  $\Theta$  correspond to a Doppler and delay index, respectively. Note that the total number of nonzero elements in  $\Theta$  is  $P$ . At the receiver, the matched filtering based on  $u(t)$ , the orthogonality within this specific TF region defined by the digital implementation of the (signal)-th TF grid. A single element of  $\Theta$ , denoted by  $\Theta_{m,n}(\tau, \nu, k, l)$ , be equal to the gain  $h_{\tau,\nu}$  of the path whose delay and Doppler are  $\tau T_0$  and  $\nu T_0$ , respectively. Note that the total number of symbols each having  $N$  subcarriers. Therefore it only applies to a local region in the TF domain. Since MC modulation has a limited number of symbols and subcarriers, the orthogonality within this specific TF region defined by the digital implementation of the (signal)-th TF grid. A single

resultantly we can further subdivide the design of ODDM from MC modulation by taking the TF DoF  $\min\{M, N\}$  of the practical signal into account.

Without loss of generality, let us consider the TF region in Fig. ??, where the bandwidth and duration are  $B$  and  $T_x$ , respectively. It is widely understood that for a signal contained in this region, its DoF is bounded by  $BT_x$ , which can be achieved by using the prolate spheroidal wave functions [?]. In other words, we can transmit up to  $[BT_x]$  digital symbols, by carrying them using the PSW functions. However, for  $PSW \leq M-1$ . Then, the noise-free IQ relation of ODDM over the ESDD channel can be written as

$$\mathbf{y} = \mathbf{H}\mathbf{x}, \quad (43)$$

where the DD domain channel matrix  $\mathbf{H}$  is given by

$$\mathbf{H}_0^L \quad \mathbf{H}_{L-1}^L \mathbf{D} \quad \dots \quad \dots \quad \mathbf{H}_0^L \mathbf{D}$$

Analogous to (??) and (??), the  $\mathbf{H}_0^L$  (bi)orthogonal pulse design problem taking the TF constraints of the signal, namely the limited number of symbols and subcarriers, into account is to find specific WH subsets  $(g, \mathcal{T}, \mathcal{F}, M, N)$  and  $(\gamma, \mathcal{T}, \mathcal{F}, M, N)$  that satisfy the orthogonal condition of

$$\langle g_{m,n}, g_{m,n} \rangle = \delta(m-m)\delta(n-n), \quad m, \bar{m} \in \mathbb{Z}_M, n, \bar{n} \in \mathbb{Z}_N \quad (48)$$

or the biorthogonal condition of

$$\langle g_{m,n}, \mathbf{H}_m^L \rangle \equiv \delta(m-\bar{m})\delta(\bar{n}K+\bar{l}), \quad \bar{m} \in \mathbb{Z}_M, \bar{n}, \bar{l} \in \mathbb{Z}_N, \quad (49)$$

$$\text{where } \mathbf{D} = \text{diag}\left\{1, e^{-j\frac{2\pi}{N}}, \dots, e^{-j\frac{2\pi(N-1)}{N}}\right\}, \quad (46)$$

$$\mathbb{Z}_M = \{0, 1, \dots, M-1\}, \quad \mathbb{Z}_N = \{0, \dots, N-1\}. \quad (50)$$

and the  $N \times N$  cyclic permutation matrix is formulated. Here, the index of subcarriers  $\{-N/2, \dots, 0, \dots, N/2-1\}$  is changed to  $\{0, \dots, N-1\}$  for simplifying the notation, which corresponds to a half-bandwidth shift of the carrier frequency  $f_c$ . This will not affect the analysis of (bi)orthogonality.

Since (??) and (??) only consider a focal region in the TF domain, we term them as the sufficient orthogonal condition and sufficient biorthogonal condition, respectively. Further as an  $MN \times MN$  block-circulant-like matrix, the DD domain channel matrix  $\mathbf{H}$  in (??) represents the linear combination between  $X[m, n]$  and the ESDD channel  $h(\tau, \nu)$ . Upon using the DDOP  $u(t)$  of Fig. ?? as the transmit and receive prototype pulses, ODDM becomes capable of outperforming the OTFS in terms of both its OOBE and bit error rate [?], [?]. It is noteworthy that with the DDOP namely the pulse-chain  $u(t)$ , the ODDM can be viewed as a PS-OFDM similar to precisely abridged for the sufficient ODDM orthogonal condition in (??).

The existence of the ODDM sets of (??) is analyzed by this property signaling in the spatial of  $L$  in the following of (iii) orthogonal pulses indicates how the orthogonal WH sets dominate with respect to the width of the TF region and the feed-in (NT\_0) stability (M+N) reconstruction exists this requires (R) thus motivates when we consider the TF dimension of the orthogonal

denote design principles based on the WH frame theory which will be discussed in the next section. The duality and biorthogonality theory for WH frames [2], [3], [4], we know that (Pulse Design Subject) are biorthogonal TF constraints associated with the sets  $\{g, \mathcal{T}, \mathcal{F}\}$  and  $\{\gamma, \mathcal{T}_\dagger, \mathcal{F}_\dagger\}$  are dual frames within  $(M, N)$  symbols having only one symbol per subcarrier. Therefore, the set  $\{g, \mathcal{T}, \mathcal{F}\}$  is a tight frame. To obtain the dual, since MC modulation has a limited number of symbols  $M$  and the corresponding orthogonality within  $R = T_\dagger \mathcal{F}$  region and consequently the bandwidth  $B$ . Therefore, (bi)orthogonal WH sets do not exist from  $R$ , we can reformulate the pulse design problem. The WH-FMC theory based on the results regarding (bi)orthogonal WH sets provides a solution. However, since a WH set is originally a TF without concern for general functions in  $L^2(\mathbb{R})$ , it considers the whole TF domain where the bandwidth  $\mathcal{F}$  and the corresponds to the signal with the limit of bandwidth and duration to make this possible in given  $\mathcal{T}_\dagger$ . Its DOFs must be bounded by  $B\mathcal{F}$ , the number of symbols  $M$  and the number of subcarriers  $N$  to be shifted freely. In other words, we can transmit a result  $g(t)$  in  $B\mathcal{F}$  by sighted by  $\mathcal{F}$  and trying to achieve using global PSW orthogonality. However, the PSW subbands must have a complex sinusoidal based structure required by MC modulation, on the hand, the MC modulations can not achieve the global (bi)orthogonality in (22) and (23) we only have to consider the sufficient (bi)orthogonality in (22) and (23) to satisfy the perfect reconstruction condition for duration symbols with  $N$  and carriers corresponding to a MC subband under the constraint of other signal. Apparently, and that achieves the global  $B\mathcal{F}$  orthogonality, form the cos-orthogonal WH subset of bandwidths efficiently only require a WH subset to satisfy the sufficient (bi)orthogonality. It is global and sufficed by the WH frame theory for the WH set. In fact, the pulses parameterized by not only  $\mathcal{T}$  and  $\mathcal{F}$  but also by  $M$  and  $N$  can also achieve the sufficient orthogonality design problem taking the TF constraints of the signal, namely the limited number of symbols and subcarriers, into account. Orthogonality with respect to  $\mathcal{F}$  subsets  $\{g, \mathcal{T}, \mathcal{F}, M, N\}$  and  $\{\gamma, \mathcal{T}_\dagger, \mathcal{F}_\dagger, N\}$  that satisfies the orthogonal  $\langle g_{m,n}, g_{m,n} \rangle$  and investigate the orthogonality with respect to the frequency resolution  $\mathcal{F}$  first. We want to find  $g(t)$  that can achieve the  $\langle g_{m,n}, g_{m,n} \rangle = \delta(m-m)(n-n)$ ,  $m, n \in \mathbb{Z}_m, n, \bar{n} \in \mathbb{Z}_N$ , orthogonality among  $g(t-mT)e^{j2\pi n \mathcal{F}(t-mT)}$  with a given  $n$  but variable  $m$ , where  $0 \leq t \leq T_g$  and  $T_g = T = 1/\mathcal{F}$ . Without loss of generality, let  $m = 0$ , we can obtain the following results:  $\langle g_{m,n}, g_{m,n} \rangle = \delta(m-\bar{m})\delta(n-\bar{n})$ ,  $m, \bar{m} \in \mathbb{Z}_m, n, \bar{n} \in \mathbb{Z}_N$ , (49)

F1) Unbounded  $n$  ( $n \in \mathbb{Z}$ ):  $g(t)$  is the rectangular pulse where  $H_T(t)$ , which is independent of  $N$ .

F2) Bounded  $n$  ( $|n| \leq 1, N-1 \leq |n| \leq N$ ): We have the following proposition:

Here, the index of subcarriers  $\{-N/2, \dots, 0, \dots, N/2-1\}$  Proposition 2. When  $g(N)$  is a unit energy periodic function with a period of  $\mathcal{T}$  for  $0 \leq t \leq T_g$  and  $T_g < T$ , it satisfies the orthogonality property. This will not affect the analysis of (bi)orthogonality.

$$\langle g_{g,g}(0, n\mathcal{F}), g(t) e^{j2\pi n \mathcal{F}t} \rangle = \delta(n). \quad (53)$$

Since (53) and (54) only consider a local region in the TF domain, we term them as the sufficient orthogonal condition and sufficient biorthogonal condition, respectively. ■ Furthermore, because of

<sup>6</sup>A WH frame is called tight if its lower and upper frame bounds are the same.

where  $\bar{m} = m - m$  and  $\bar{n} = n - n$ , the sufficient orthogonal condition in (53) is equivalent to

$$g(t) \xrightarrow{N} \mathcal{A}_{g,g}(mT, n\mathcal{F}) = \delta(\bar{m})\delta(\bar{n}), \quad (52)$$

for  $|m| \leq M-1, |\bar{m}| \leq N-1$ . Similar results can be obtained for the sufficient biorthogonal condition in (54).

In the context of TFA, WH sets are used for analyzing finite-energy signals lying in the space of  $L^2(\mathbb{R})$ . For accurate analysis, the WH sets have to be WH frames. Proposition ?? indicates that once there is a constraint imposed which are complete or overcomplete WH sets with a certain guaranteed numerical stability of reconstruction and this requires  $R \leq 1$  [2, 7]. When a WH set  $\{g, \mathcal{T}, \mathcal{F}\}$  is a WH frame, we can denote it as  $\{g, \mathcal{T}_\dagger, \mathcal{F}\}$  by replacing as long as  $g(t)$  is a periodic function satisfying the above round brackets with curly brackets. Let  $\mathcal{T}_\dagger = 1/\mathcal{F}$  and conditions, regardless of its bandwidth  $B_g$ , it can achieve the orthogonality among  $N$  subcarriers. Considering the case of  $\{g, \mathcal{T}_\dagger, \mathcal{F}_\dagger\}$  where  $B_g$  is proportional to  $\mathcal{F}$  and the total bandwidth of  $\{g, \mathcal{T}_\dagger, \mathcal{F}_\dagger\}$  are biorthogonal if and only if the associated signal is about  $N\mathcal{F}$ . Proposition ?? actually decouples the WH sets  $\{g, \mathcal{T}_\dagger, \mathcal{F}_\dagger\}$  and  $\{g, \mathcal{T}_\dagger, \mathcal{F}\}$  are dual frames, while relation between  $B_g$  and  $\mathcal{F}$ . An example of such a function  $(g, \mathcal{T}, \mathcal{F})$  is orthogonal if and only if the associated WH set  $\{g, \mathcal{T}_\dagger, \mathcal{F}_\dagger\}$  is a tight frame. To obtain the dual frames  $\{g, \mathcal{T}_\dagger, \mathcal{F}_\dagger\}$  and  $\{\gamma, \mathcal{T}_\dagger, \mathcal{F}_\dagger\}$  or the tight frame  $\{g, \mathcal{T}_\dagger, \mathcal{F}_\dagger\}$ , the corresponding JTFR has to satisfy  $R_\dagger = \mathcal{T}_\dagger \mathcal{F}_\dagger \leq 1$  and similarly  $R$  consider a fixed  $\mathcal{T}_\dagger$  therefore, (49) in regard to WH orthogonality exist respect to the time resolution  $\mathcal{T}$ . Our target now is to find a signal  $g(t)$  that can achieve the global (bi)orthogonality among  $N$  subcarriers. However, since a WH set fixed originally a TF set, all the functions have the following straightforward for the signal without the limit of bandwidth and duration  $T$ . To make this possible, given  $T_g \leq T$  and  $\mathcal{F}, g(t)$  must be independent of the number of symbols  $M$  and the number of subcarriers  $N$  to be shifted freely over the whole TF domain. As a result,  $g(t)$  is designed based only where these subpulses achieve the global (bi)orthogonality in (53) and (54) and therefore bounded by the JTFR limit of  $R = 1$ .

Meanwhile, when  $n = 0$ , we have another solution associated

On the other hand, for MC modulations, in contrast to achieving the global (bi)orthogonality in (53) and (54), T3) Unbounded  $m$  ( $m \in \mathbb{Z}$ ): square-root Nyquist pulse we only have to consider the sufficient (bi)orthogonality in  $\langle g(t), a_{\mathcal{T}}(t) \rangle$  with  $\mathcal{T}$  being the zero-ISI interval, which is also in (53) and (54) to satisfy the perfect reconstruction condition for  $M$  MC symbols with  $N$  subcarriers.

T4) Bounded  $m$  ( $|m| \leq M-1$ ):  $g(t)$  is a pulse-train being made up of  $N > 1$  square-root Nyquist subpulses  $a_{\mathcal{T}}(t)$  of the signal. Apparently,  $g(t)$  that achieves the global (bi)orthogonality can form a (bi)orthogonal WH subset.

However, since we really only require a WH subset to satisfy the sufficient (bi)orthogonality, it is not necessarily bounded by the WH frame that give for the WH resolution, the key is achieving the orthogonality among  $N$  subcarriers by employing square-root Nyquist pulses whose zero-ISI interval  $\mathcal{T}$ . Also, for the case of the pulse train in T2) and T4) corresponding to the sufficient orthogonality, the subpulses

Let us consider a fixed  $m$  and variable  $n$  in  $g_{m,n}$  and have to be temporally spaced by  $M\mathcal{F}$ . At the same time, we investigate the orthogonality with respect to the frequency known from F2) that given the frequency resolution  $\mathcal{F}$ , the key resolution  $\mathcal{F}$  first. We want to find  $g(t)$  that can achieve to achieving the sufficient orthogonality among  $N$  subcarriers the orthogonality among  $g(t-mT)e^{j2\pi n \mathcal{F}(t-mT)}$  with a is to form a periodic function with period  $\frac{1}{N\mathcal{F}}$ . Therefore, to achieve the sufficient orthogonality with respect to  $\mathcal{F}$  and  $\mathcal{T}$  concurrently, we can consider a combination of the conditions

in T2), T4) and F2). Furthermore, because the subpulses in T2) have much shorter duration and therefore much wider bandwidth than those in T4), the combination of T4) and F2) is preferred.



Given the time resolution  $\tau$  and assuming that the duration of  $a_T(t)$  obeys  $T_{a_T} < M\tau$ , it is interesting to observe that by fitting the (number of subpulses) to be  $N \leq N_0$ , the pulsed train in T4 is a periodic function that satisfies F2), if we let  $T_g = T = MN\tau$  and  $\mathcal{F} = 1/T = 1/(MN\tau)$  in F2). Further, upon given  $m$ , the variable  $n$ , where  $0 \leq t \leq T_g$  and  $T_g = T = 1/\mathcal{F}$ . Without loss of generality, let  $m = 0$ , we can obtain of (??) and achieves orthogonality with respect to  $\tau = \frac{1}{M}$  and  $\mathcal{F} = 1/(N\tau_0)$ , where  $R = 1/(MN) \ll 1$ .

F1) As illustrated combining the pulse is then retimed and rescaled by the orthogonality is independent of  $\Delta N$ . Doppler resolution, F2) Bousfield's theorem (Nyquist pulse). We will have the following proposition:

Proposition 2: Due to the delay resolution, we can bypass the JTFR limit of  $R \geq 1$  for global (bi)orthogonality to achieve sufficient orthogonality with  $R \ll 1$ . Compared to the traditional WH set based principles, the WH subset based satisfies the orthogonal property of principles and the resultant pulse-train structure may pave the way for concerning new pulse designs for MC modulations.

$$\mathcal{A}_{g,g}(0, n) = \langle g(t), g(t) \rangle_{\mathcal{M}} = \delta(n). \quad (53)$$

## for General NDDOP and Sufficient Biorthogonality

**Prop. See Appendix A.** The above result of sufficient orthogonality is based on the Proposition V indicates that once there is  $M\mathcal{T}$ . Recall that the orthogonality of the DDOP in (2) is also subject to a similar duration constraint of  $T_s \leq T_{DDOP}$  (equivalently  $20 \leq M$ ). In practice, it is desirable to relax this constraint for the sake of flexible design. In the following, we will show that this extension can be relaxed by introducing the cyclic extension bandwidth  $B_g$ , which leads to a general DDOP design.

When  $T_s > T_{DDOP}$  (no longer a period function with a period of  $T_s$  during  $[0, NT_s]$ ), which is required to satisfy the orthogonality with respect to  $\mathcal{F} = \frac{1}{NT_s}$ . This observation inspires us to use a cyclically extended version of  $y(t)$  namely  $y_{ce}(t)$  as the transmit pulse, while the receive pulse is still  $u(t)$ , corresponding to a biorthogonality condition. Furthermore, because the cross ambiguity function  $A_{u_c, y_{ce}}(\cdot)$  is C. Orthogonality with Respect to  $\mathcal{F}_{ce} = e^{j2\pi \frac{n}{M}(t-m\frac{\mathcal{T}}{M})}$ , the problem to satisfy the orthogonality with respect to  $\mathcal{F}_{ce}$  becomes how  $y_{ce}(t)$  can have the specified periodicity within resolution  $\mathcal{T}$ . Our target now becomes that of finding the range of  $u(t-m\frac{\mathcal{T}}{M})e^{j2\pi \frac{n}{M}(t-m\frac{\mathcal{T}}{M})}$  for  $|m| \leq M-1$ , a specific  $g(t)$  that can achieve the orthogonality among  $\mathcal{F}_{ce}$ . We then have the following proposition:

**Proposition 13.** We have the following straightforward answer to the question of isolated pulses/subpulses temporally spaced by  $T_0$ . The resultant pulse train satisfies the biorthogonality property (11) if and only if  $m \in \mathbb{Z}$ . Any  $g(t)$  with duration of  $T_a < T$ , which is independent of  $M$ .

T2) Bounded  $m_{\text{acc}, u}((m \leq M-1); y(t))$  is a pulse-train being made up of  $N > 1$  subpulses  $b_n(t), 0 \leq n \leq N-1$ , for where these subpulses are temporally spaced by  $M T_0$  cyclically end-to-end over a period of  $d(t)$ . Specifically,  $T_{\text{acc}}(t)$  is a periodic function with period  $T_0$  during  $- (M-1) \frac{T_0}{N} \leq t \leq (M-1) \frac{T_0}{N}$ . Meanwhile, when  $n = 0$ , we have another solution associated with temporally overlapped pulse/subpulses:

T3) Probing Sidelobe Appendix BZ : square-root Nyquist pulse  
 Note that with probing the position interval, no dependence on  $T_p$ , which indicates that the duration constraint of  $a(t)$  in  $u(t)$

(a) b) embedded. Once the appropriate CB and CS are added, according to the  $\Sigma N$ , where the extension parameter  $b$  for CB and CS (is), when these submodels are independently sufficient, biorthogonality can be achieved as well.

## D. Sufficient Orthogonality with Respect to $\mathcal{P}$ and $\mathcal{P}'$

Given the general DDOP design given the transmit pulse of QPSK modulation becomes  $u(t)$ . When  $M \gg 2Q$ , we have  $2Q/M \approx 0$ . Then, as proved in [2], ODDM can employ the symbols is to either limit the pulse duration to be no greater than  $u(t)$  without cyclic extension ( $D=0$ ) or to employ square-root Nyquist pulses whose zero-ISI interval is  $\mathcal{T}$ . Also, for the case of the pulse FF signal in T2, T3 and T4 corresponding to the sufficient orthogonality, the subpulses have to be temporally spaced by  $MT$ . At the same time, we know from F2) that given the frequency resolution  $F$ , the key to achieving the sufficient orthogonality among  $N$  subcarriers is to form a periodic function with period  $\frac{1}{F}$ . Therefore, to achieve the sufficient orthogonality with respect to  $F$  and modulation, we need both the TD and FD representations of its  $T$ , concurrently. We can consider a combination of the transmit pulse. In the following, we will derive  $U(t)$ , namely conditions in T2), T3) and T4). Furthermore, because the FD representation of  $u(t)$  corresponding to the case of subpulses in T2) have much shorter duration and therefore  $D=0$ , as we usually have  $M \gg 2Q$  in practice.

much wider bandwidth than those in T4), the combination of T4 and F2 is preferred.

Given the time resolution  $\mathcal{T}$  and assuming that the duration of  $a_{\mathcal{T}}(t)$  obeys  $a_{\mathcal{T}}(t) = \sum_{n=-\infty}^{\infty} \delta(t - nT_0)$ , it is interesting to observe that by letting the number of subpulses to be  $N = N$ , the pulse-train in T4) is a periodic function that satisfies F2), if we let  $T_g = T = MN\mathcal{T}$  and  $\mathcal{F} = 1/T = 1/(MN\mathcal{T})$  in F2). Further, upon substituting  $\frac{T_0}{M}$  into  $\mathcal{T}$ , the pulse-train becomes the DDOP  $u(t)$  of (??) and achieves the orthogonality with respect to  $\mathcal{T} = \frac{T_0}{M}$  and  $\mathcal{F} = 1/(NT_0)$ , where  $\mathcal{R} = 1/(MN) \ll 1$ .

As a result, by combining the pulse-train structure required by the orthogonality with respect to the Doppler resolution and the square-root Nyquist pulse required by the orthogonality with respect to the delay resolution, we can bypass the JTDR limit of  $\mathcal{R} \geq 1$  for global (bi)orthogonality to achieve sufficient orthogonality with  $\mathcal{R} \ll 1$ . Compared to the traditional WH set based principle where  $\hat{u}(t) = \bar{u}(t) \times \Pi_{NTD}(t + \frac{T_0}{2})$  and  $*$  denotes convolution, the WH subset based principles and the resultant convolution. Since the multiplication and convolution in the TD pulse-train structure may pave the way for conceiving new correspond to the convolution and multiplication in the FD, pulse designs for MC modulations, respectively, we have

## E(General DDOP) and Sufficient Biorthogonality

The above result of sufficient orthogonality is based on the appropriate duration of  $a_T(t)$  namely  $T_{aT} < MT$ . Recall that the orthogonality of the DDOP in (??) is also subject to a similar duration constraint of  $T_a \ll T_0$  (equivalently  $2Q \ll M$ ). In practice, it is desirable to relax this constraint for the sake of flexible design. In the following we will show that this duration constraint ( $T_a$  can be relaxed by 2) is due to the cyclic extension which leads to Wigner-Doob energy. To prove this, let  $M$  be an even number. Then the derivative of (6) is no longer periodic in  $t$  due to the period  $\pi T_0$  of the rectangular window function. This observation becomes clear if we cyclically extend  $Sinc(JNT_0)$  to  $\infty$  and consider the corresponding derivative. The resulting derivative is given by

version(t) of  $u(t)$  namely  $u_{ce}(t)$ , as the transmit pulse, while the receive pulse is still  $u(t)$ ; corresponding to a biorthogonality condition. Furthermore, because the cross ambiguity function  $\mathcal{A}_{u_{ce}, u}(t)$  is calculated between  $u_{ce}(t)$  and  $u(t - m\frac{T_0}{M})e^{j2\pi\frac{n}{NT_0}(t-0\frac{T_0}{M})}$ , the problem to satisfy the orthogonality with respect to  $\mathcal{F} = \frac{1}{NT_0}$  becomes how  $u_{ce}(t)$  can have the specified periodicity within the range of  $u(t - m\frac{T_0}{M})e^{j2\pi\frac{n}{NT_0}(t-0\frac{T_0}{M})} \leq (N-1)T_0$  for  $|m| \leq M-1$ . We then have the following proposition:

**Proposition 3.** Let a pulse-train  $u(t)$  be made up of  $N$  square-root Nyquist pulses  $a(t)$  which are temporally spaced by  $T_0$ . The resultant pulse train satisfies the biorthogonality property of

$$\text{Fig. 12. Derivation of } \mathcal{A}_{u_{ce}, u}\left(\frac{m}{M}, n\frac{1}{NT_0}\right) = \delta(m)\delta(n), \quad (54)$$

for  $|m| \leq M-1$  and  $|n| \leq N$  with where  $u_{ce}(t)$  is a cyclically extended version of  $u(t)$ . Specifically,  $u_{ce}(t)$  is a periodic function with period  $T_0$  during  $-(M-1)\frac{T_0}{M} \leq t \leq (MN-1)\frac{T_0}{M} + T_0$  with different subpulses  $a(t)$ . In fact, we can choose the subpulse to determine the envelope of the FD representation of the pulse train, which corresponds to the bandwidth of the pulse train. Meanwhile, we are also free to choose  $N$  and  $T_0$  for beneficially manipulating the FD representation of the pulse train under the envelope, which is  $U(f)$ .

**Note that the proof of Proposition 3 does not depend on  $T_0$ , which indicates that the duration constraint of  $a(t)$  in  $u(t)$  can be removed. Once the appropriate CP and CS are added in accordance with (17), where the extension parameter for CP and CS is  $D = [T_a/T_0] = [2Q/M]$ , the desired sufficient biorthogonality can be achieved as well.**

**2) DDOP as Virtual 2D Pulse:** Being a continuous-time function, a pulse can be described either by its TD representation

VII or FD representation  $G(f)$  where these two representations are tightly bound by the (inverse) Fourier transform and

Given the general DDOP design, the transmit pulse therefore dependent on each other. This dependency is exactly of ODDM modulation becomes  $u_{ce}(t)$ . When  $M > 2Q$  the reason why the TFA of the pulse has a lower bound (Gabor limit) of  $1/(4\pi)$  corresponding to the Heisenberg uncertainty principle. As a result, although we may be able to present the TF localization of a pulse in the TF domain by illustrating its

A) **TF Signal Localization**: The time signal localization via plays a important role in the interplay of modulations. Therefore, we cannot form a 2D TF signal localization of GR-ODDM given that Fig. 12 depicts its  $g(t, f)$  in other words, a pulse is always a JTFB function in conventional TF domain. To understand the TF signal localization of a pulse, we need to understand the dual variable  $\tau$  and FD representation of it, namely the time-pulse and frequency localizations of the pulse in the FD domain are independent of each other. This is the reason why the FD representation of  $u(t)$  corresponding to the time domain, and we do not have 2D impulse responses for LTV channels, represented by the spreading function domain.

**Representation of DDOP:** It is widely exploited that the FD representation of a pulse having a pulse-train structure may be considered as a "virtual" 2D pulse to match the signal to the channel. For example, the intervals between the subpulses and the time during the interval may be considered as two potential variables of the pulse. For instance, in this 2D pulse, the virtual structure of the pulse train in the FD which have been widely used in radar waveform design [2], [3]. In particular, for the pulse-train  $u(t)$ , although its subpulse  $a(t)$  has a tightly bound pair of time variable and frequency variable  $f$ , we can repeat the subpulse  $a(t)$  and

It is interesting to observe that the DDOP can be obtained from  $\dot{u}(t)$  by applying a rectangular window  $\Pi_{NT_0}(t + \frac{T_0}{2})$  followed by a filter with the impulse response  $a(t)$ . Then, we have

$$\text{Fourier transform} \quad U(f) = \dots u\left(t + \frac{T_0}{2}\right) = \dot{u}(t) * a(t), \quad (57)$$

where  $\dot{u}(t) = \dot{u}(t) * \Pi_{NT_0}(t + \frac{T_0}{2})$  and  $*$  denotes convolution. Since the multiplication and convolution in the TD correspond to the convolution and multiplication in the FD, respectively, we have

$$\begin{aligned} U(f) &= e^{-j2\pi f\frac{T_0}{2}} A(f) U(f) \\ &= e^{-j2\pi f\frac{T_0}{2}} A(f) \left( \tilde{U}(f) * e^{-j2\pi f\frac{(N-1)T_0}{2}} \text{Sinc}(fNT_0) \right), \\ &= \frac{e^{-j2\pi f\tilde{T}_0}}{T_0} A(f) \sum_{m=-\infty}^{\infty} e^{j2\pi \frac{m(N-1)}{2}} \text{Sinc}(fNT_0 - mN), \end{aligned} \quad (58)$$

where  $\tilde{U}(f) = \tilde{U}(f) * e^{-j2\pi f\frac{(N-1)T_0}{2}} \text{Sinc}(fNT_0)$ ,  $\tilde{T}_0 = (T_a + (N-1)T_0)/2$  and  $A(f)$  is the Fourier transform of  $a(t)$ .

Without loss of generality, let  $M$  be an even number. Then, the derivation of  $U(f)$  is graphically illustrated in Fig. 13, where the phase terms are omitted and the shapes of  $\text{Sinc}(fNT_0 - mN)$  are truncated for the purpose of display [7], [8]. Now, it becomes clear that  $\text{Sinc}(fNT_0 - mN)$  and  $A(f)$  correspond to the orthogonality with respect to  $\mathcal{F} = \frac{1}{NT_0}$  and  $\mathcal{T} = \frac{T_0}{M}$ , respectively.

The operations in Fig. 13 can be extended straightforwardly to other pulse-trains with different subpulses  $a(t)$ . In fact, we can choose the subpulse to determine the envelope of the FD representation of the pulse-train, which corresponds to the bandwidth of the pulse-train. Meanwhile, we are also free to choose  $N$  and  $T_0$  for beneficially manipulating the FD representation of the pulse train under the envelope, which is  $\hat{U}(f)$ .

**2) DDOP as Virtual 2D Pulse:** Being a continuous-time function, a pulse can be described either by its TD representation  $u(t)$  or FD representation  $G(f)$ , where these two representations are tightly bound by the (inverse) Fourier transform and therefore dependent on each other. This dependency is exactly the reason why the TFA of the pulse has a lower bound (Gabor limit) of  $1/(4\pi)$  corresponding to the Heisenberg uncertainty principle. As a result, although we may be able to present the TF localization of a pulse in the TF domain by illustrating its time and frequency representations together as shown in Fig. 12, the time signal localization via plays a important role in the interplay of modulations. Therefore, we cannot form a 2D TF signal localization of GR-ODDM given that Fig. 12 depicts its  $g(t, f)$  in other words, a pulse is always a JTFB function in conventional TF domain. To understand the TF signal localization of a pulse, we need to understand the dual variable  $\tau$  and FD representation of it, namely the time-pulse and frequency localizations of the pulse in the FD domain are independent of each other. This is the reason why the FD representation of  $u(t)$  corresponding to the time domain, and we do not have 2D impulse responses for LTV channels, represented by the spreading function domain.

**Representation of DDOP:** It is widely exploited that the FD representation of a pulse having a pulse-train structure may be considered as a "virtual" 2D pulse to match the signal to the channel. For example, the intervals between the subpulses and the time during the interval may be considered as two potential variables of the pulse. For instance, in this 2D pulse, the virtual structure of the pulse train in the FD which have been widely used in radar waveform design [2], [3]. In particular, for the pulse-train  $u(t)$ , although its subpulse  $a(t)$  has a tightly bound pair of time variable and frequency variable  $f$ , we can repeat the subpulse  $a(t)$  and

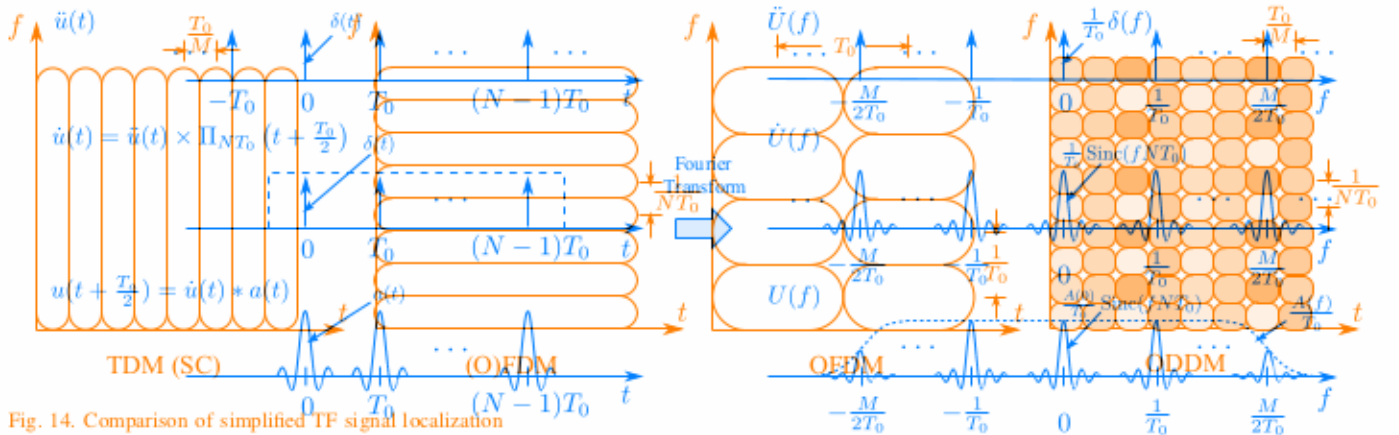


Fig. 14. Comparison of simplified TF signal localization

### Fig. 12. Derivation of $U(f)$

respect to the delay resolution  $\frac{T_0}{M}$  and the Doppler resolution  $\frac{1}{NT_0}$  is achieved by  $a(t)$  in  $u(t)$  and  $\text{Sinc}(fNT_0)$  in  $U(f)$ , respectively. With the aid of  $u(t)$  and  $U(f)$ , the simplified TF signal localization of DDOP having a pulse train structure may be considered as a "virtual" 2D pulse to match the signal to the channel.

3) *Comparison of TF Signal Localization.* To transmit  $MN$  QAM symbols, an MC modulation scheme employs  $MN$  time during an interval may be considered as two potential variables of the pulse train or the virtual 2D pulse. This is similar to slow time and fast time, which have been widely used in radar waveform design [2], [3]. In particular, for the pulse train  $u(t)$ , although its subpulse  $a(t)$  has a tightly bound pair of time variable  $t$  and frequency variable  $f$ , we have to repeat the subpulse  $a(t)$  and introduce an extra time variable  $t$ , the minimum unit of which is  $T_0$ . By letting  $t = \tau + t$ , we can virtually represent  $u(t)$  as a 2D function  $u(\tau, t)$  subject to the following constraints:

- 1) For SC modulation, which is a time-division multiplexing scheme, the  $MN$  QAM symbols are conveyed by  $MN$  square-root Nyquist pulses for the zero-ISI interval  $\frac{T_0}{M}$ . The pulses are orthogonally overlapped in the TD. (59)
- 2) For a frequency-division multiplexing (FDM) scheme, such as for example OFDM associated with frequency resolution of  $\frac{1}{NT_0}$ ,  $MN$  QAM symbols are conveyed by  $MN$  rectangular pulses  $\Pi_{NT_0}(t)$  modulated by  $MN$  subcarriers, respectively. The pulses are inseparably overlapped in the TD however they are orthogonally overlapped in the FD. The last two constraints in (??) actually correspond to  $\hat{U}(f)$ , the FD representation of the pulse train under the envelope of  $\frac{1}{NT_0}$  and time resolution  $T_0$ ,  $MN$  QAM symbols are we mentioned before.

It should be noted that introducing  $t$  does not mean symbol has  $M$  rectangular pulses  $\Pi_{T_0}(t)$  modulated by  $M$  subcarriers, respectively. Since  $N$  OFDM symbols are isolated in the TD, the inter-symbol pulses are not overlapped either in the TD or in the FD while the signal to be equally spaced distributed in both the TD and intra-symbol pulses are inseparably and orthogonally overlapped in the TD and FD, respectively.

- 4) For ODDM having a frequency resolution of  $\frac{1}{NT_0}$  and a time resolution of  $\frac{T_0}{M}$ ,  $MN$  QAM symbols are conveyed by  $M$  pulse trains  $u(t)$  modulated by  $N$  subcarriers, respectively. These pulses are overlapped orthogonally both the TD and FD.

3) *Comparison of TF Signal Localization.* The bandwidth of  $MN$  QAM symbols, measured full-duplexing at the bandwidth of  $MN$  frequency bins corresponding to the sets of TF Rho and

overlapped in both the TD and FD. Recall that for the TF region is bounded by  $B$  and  $T_x$ , we have a DoF around  $BT_x$ . Then for a given  $M$  and  $N$ , we can calculate the necessary  $B$  and  $\frac{M}{2T_0}$  for each modulation scheme and obtain their bandwidth efficiencies accordingly.

### B. Bandwidth Efficiency

Let the square-root Nyquist pulse be a root raised cosine pulse with roll-off factor  $\rho$ . Upon recalling that  $T_a = 2Q\frac{T_0}{M}$ , we have

$$\begin{aligned} \eta_{\text{TDM}} &= \frac{\int_{-\infty}^{\infty} |\Pi_{NT_0}(t)|^2 dt}{\int_{-\infty}^{\infty} |\Pi_{NT_0}(t)|^2 dt + \int_{-\infty}^{\infty} |\Pi_{NT_0}(t)|^2 dt} \\ &= \frac{\frac{1}{M} (1 + \rho)((MN - 1)\frac{T_0}{M} + T_a)}{(1 + \rho)(1 + \frac{2Q - 1}{MN})}. \end{aligned} \quad (60)$$

For (O)FDM, because  $|\text{Sinc}(fNT_0)|$  decays as  $1/f$ , it can be treated as negligibly small beyond the  $k$ th zero crossing on both sides of the main lobe. In other words, the bandwidth of  $g(t) = \Pi_{NT_0}(t)$  is considered as  $B_g = \frac{2K}{NT_0}$ . Then, we have

$$\eta_{\text{OFDM}} = \frac{MN}{B_g NT_0} = \frac{1}{\frac{2K}{NT_0} \frac{MN}{NT_0}} = \frac{1}{MN} \quad (61)$$

results in its own TF signal localization. Based on Fig. ??, the comparison between ODDM and other modulation schemes in terms of their simplified TF signal localization

Let us now consider CP-OFDM. Because of the delay spread of the channel,  $u(t)$  is  $\Pi_{NT_0}(t)$  and  $T_a = \frac{L}{T_0}$ ; Therefore, we have

we should note that for ODDM,  $M$  has to be a large enough integer to have a reasonable extension parameter  $D = |2Q| \frac{M}{(1 + \rho)(1 + \frac{2K - 1}{MN})}$  for the general DDOP. From Fig. ??, one can observe that:

$$\eta_{\text{CP-OFDM}} = \frac{MN}{B_g NT_0} = \frac{1}{\frac{2K}{NT_0} \frac{MN}{NT_0}} = \frac{1}{MN} \quad (62)$$

- 1) For SC modulation, which is a time-division multiplexing scheme, the  $MN$  QAM symbols are conveyed by  $MN$  square-root Nyquist pulses for the zero-ISI interval  $\frac{T_0}{M}$ . The pulses are orthogonally overlapped in the TD.

2) For a frequency-division multiplexing (FDM) scheme, such as for example OFDM associated with frequency resolution of  $\frac{1}{NT_0}$ ,  $MN$  QAM symbols are conveyed by  $MN$  rectangular pulses  $\Pi_{NT_0}(t)$  modulated by  $MN$  subcarriers, respectively. The pulses are inseparably overlapped in the TD. Due to its good TF localization, the RRC pulses modulated by spreading code/sequence were adopted by the third generation mobile communication system orthogonal multiplexed communications.

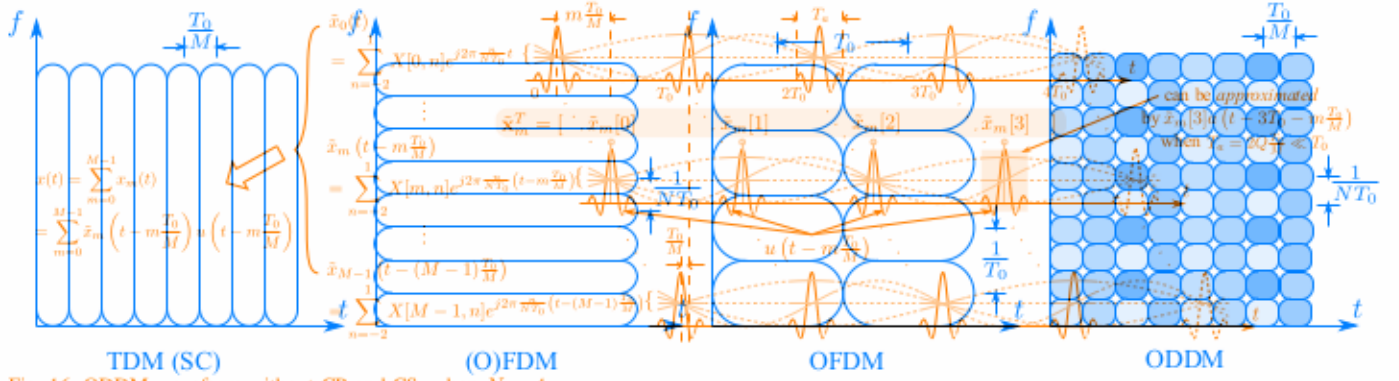
Fig. 16. ODDM waveform without CP and CS, when  $N = 4$ .

Fig. 14. Comparison of simplified TF signal localization

- 3) For conventional OFDM having a frequency resolution of  $\frac{1}{T_0}$  and time resolution  $T_0$ ,  $MN$  QAM symbols are conveyed by  $N$  OFDM symbols, where each OFDM symbol has  $M$  rectangular pulses  $\Pi_{T_0}$  modulated by  $M$  subcarriers, respectively. Since  $N$  OFDM symbols are isolated in the TD, the inter-symbol pulses are not overlapped either in the TD or in the FD, while the intra-symbol pulses are inseparably and orthogonally overlapped in the TD and FD, respectively.
- 4) For ODDM having a frequency resolution of  $\frac{1}{NT_0}$  and a time resolution of  $\frac{T_0}{M}$ ,  $MN$  QAM symbols are conveyed by  $M$  pulse trains  $u(t)$  modulated by  $N$  subcarriers, respectively. These pulses are overlapped orthogonally in both the TD and FD.

Fig. 15. bandwidth efficiency of modulation schemes,  $L = 20$ . Since the overlapping of pulses is the key to high bandwidth efficiency [?], [?], it is meaningful to investigate the bandwidth efficiency of the ODDM modulation, the When  $2Q \ll M$ , we can let  $D = 0$ . Then, the ODDM frame pulses of which are overlapped in both the TD and FD, only needs a single CP corresponding to the delay spread of the channel. For such an ODDM frame with CP only (CP, ODDM), we have a DoF around  $BT_x$ . Then, for a given  $M$  and  $N$ , we can calculate the necessary  $B$  and  $T_x$  for each modulation scheme and obtain their bandwidth efficiencies accordingly. 
$$\eta_{CP, ODDM} = \frac{1}{(1 + \rho + \frac{N-1}{MN})(1 + \frac{L+2Q-1}{MN})}. \quad (64)$$

Considering  $\frac{1}{T_0} = 15\text{kHz}$  and the Extended Vehicular A channel model of [?] associated with delay spread 2510ns, a bandwidth efficiency comparison of these modulation schemes is shown in Fig. ??, where  $M = 312$ ,  $L = 20$ , and  $K = 11$  corresponding to the 99% fractional power containment bandwidth. One can see that ODDM has similar bandwidth efficiency to SC modulation. For a moderately large  $N$  and an appropriate  $M$ , ODDM has better bandwidth efficiency than CP-OFDM, while the (O)FDM with  $\mathcal{F} = \frac{1}{NT_0}$  has the highest bandwidth efficiency. Note that the (O)FDM associated with  $\mathcal{F} = \frac{1}{NT_0}$  has  $MN$  subcarriers and therefore it is extremely “expensive” to implement. For (O)FDM, because  $|\text{Sinc}(fNT_0)|$  decays as  $1/f$ , it can be treated as negligibly small beyond the  $K$ th zero-crossing.

### C. Implementation Methods

Being a standard MC modulation, ODDM can be implemented straightforwardly via the analog and digital approaches mentioned in Section ?? . In particular, we can substitute

on both sides of the main lobe. In other words, the bandwidth of  $g(t) = \text{IFFT}_{NT_0}(t)$  is considered as  $B_g = 2K\frac{1}{NT_0}$ . Then, we have

$$\eta_{(O)FDM} = \frac{MN}{(\frac{MN-1}{NT_0} + \frac{2K}{NT_0})NT_0} \stackrel{\text{filtering}}{=} \frac{1}{1 + \frac{2K-1}{MN}}. \quad (61)$$

Let us now consider CP-ODDM. Because of the delay spread of the channel,  $g(t)$  is  $\Pi_{T_0+T_{cp}}x(t)$  and  $T_{cp} = L\frac{T_0}{M}$ . Therefore, we have

$$\begin{aligned} & \left[ \begin{array}{c} X[0, 0] \\ X[0, \frac{N}{2}-1] \\ \vdots \\ X[m, \frac{N}{2}-1] \\ X[m, -\frac{N}{2}] \\ \vdots \\ X[M-1, -1] \end{array} \right] \xrightarrow{\text{N-point IDFT}} \left[ \begin{array}{c} x_0(t) \\ \vdots \\ x_m(t) \\ \vdots \\ x_{M-1}(t) \end{array} \right] \xrightarrow{\text{filtering/pulse-shaping}} \left[ \begin{array}{c} x_0^T \\ \vdots \\ x_M^T \\ \vdots \\ x_{M-1}^T \end{array} \right] \xrightarrow{\text{TMX}} \left[ \begin{array}{c} 1 \\ \vdots \\ x(t) \\ \vdots \\ 1 \end{array} \right]. \end{aligned} \quad (62)$$

Fig. 17. Approximate implementation of ODDM. For ODDM, because the cyclic extension of  $u(t)$  is equivalent to the frame based CP and CS, we have

$$\begin{aligned} \mathcal{T} &= \frac{T_0}{M} \text{ and } \mathcal{F} = \frac{1}{NT_0} \text{ or } T = NT_0 \text{ into Figs. ??-??, and} \\ &\text{replace } g(t) \text{ by } \frac{NT_0}{T_0} \text{. However, due to the long duration } \frac{(M+L+2Q-1)}{M}T_0, \text{ these direct implementations have a high complexity, even if} \\ &\text{we generate } \bar{x}_m(t) \text{ using the IFFT}_{M+L+2Q-1}. \end{aligned} \quad (63)$$

Figure ?? shows an ODDM waveform without CP and CS. When  $2Q \ll M$ , we can let  $D = 0$ . Then, the ODDM frame only needs a single CP corresponding to the delay spread of the channel. For such an ODDM frame with CP only (CP, ODDM), we have. When  $T_a \ll T_0$ , it has been proved in [?, Appendix A] that instead of using  $u(t - m\frac{T_0}{M})$ -based pulse shaping, we can generate the discrete samples  $\bar{x}_m^T$  and then filter them with  $a(t)$  to approximate  $x_m(t)$ . For example, the fourth segment of  $x_4$  (15kHz) can be approximately generated by filtering/pulse shaping  $\bar{x}_4$  with  $a(t)$  as shown in Fig. ??, This approximation is actually *prior-informed* for the modulation as long as  $T_a \ll T_0$ . In Fig. ??, we have ODDM approximated by  $N$  filtered OFDM, where the  $N$  filter is a *delayed* filter to retain the bandwidth. One can see that ODDM has induced bandwidth loss. See detailed explanation in Remarks 2 and 4 of [?]. For a moderately large  $N$  and an appropriate  $\rho$ , ODDM has better bandwidth efficiency than CP-ODDM, while the (O)FDM with the highest complexity implementation and ODDM efficiency in Note ?? that the (O)FDM with filter pulse shaping is simply  $N$  subcarriers and the  $M$  bandwidths are expensive. To implement  $a(t)$ , we can exchange the order of the TMX

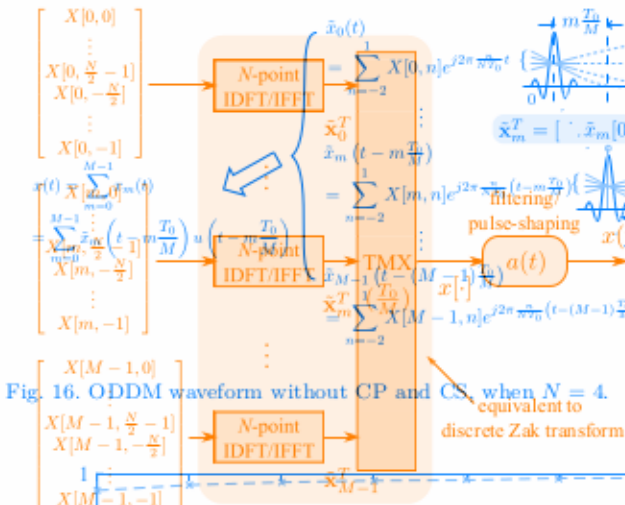


Fig. 16. Simplified approximate implementation of ODDM

and the filters to further simplify the implementation. The resultant simplified approximate implementation of ODDM using a digital TMX and a single wideband filter is shown in Fig. ??.

It is noteworthy that the combination of  $M$  branches of  $N$ -point IDFT/IFFT having  $T_0$ -interval output samples and the  $\frac{T_0}{M}$ -interval digital TMX is equivalent to a discrete Zak transform [?]. Because a discrete-time OFDM sequence can be generated using the discrete Zak transform [?], as indicated in Remark 4 of [?] a digital namely discrete-time QTFS signal filtered or pulse-shaped by  $a(t)$  approximates the ODDM waveform. Meanwhile, it should be noted that the wideband filter  $a(t)$  can also be implemented digitally, followed by a DAC having a high enough sampling rate.

### C. Implementation Methods

#### D. Potentials for ISAC

At the time of writing, ISAC is regarded as a promising implementation for next-generation wireless communications to adequately utilize the precious spectrum [?]. In particular, we can substitute  $\mathcal{T} = T_0$  and  $\mathcal{F} = \frac{1}{M} \times T_0 \times NT$  into Fig. ??, where the backscattered signals are used for estimating object or scattering parameters such as range and velocity respectively even if no general Doppler  $(t)$  using the IFFT. Because radar sensing should be ODDM or waveform without CP and CS, sometimes even opposing requirement of waveforms proposed by a main challenge (t) the ISAC system developed in this paper is interpreted as an ODDM system with a length  $T_0$ . When  $T_a \ll T_0$ , it has been proved that the diversity of the ODDM waveform can be achieved by using a parameter  $\frac{T_0}{M}$  involving phase shifting duration and the resolution of the discrete Rayleigh channel. Then, the samples  $x_m(t)$  are then filtered with a filter  $a(t)$  to approximate forms, such as frequency domain segments of waveforms and approximately obtained by filtering/pulse-shaping capability with the filter  $a(t)$  shown in Fig. ?? of this paper. This is in line with the ISAC and actually suitable for becoming the primary pulse shape of DFRC systems [?]. As far as we are concerned, the ODDM waveform is approximated by a digital filter in ODDM, where the filter form is a wideband filter with fading diversity which creates synthesize both high diversity and Doppler resilience detailed in the subsequent section.

On the other hand, from the communications perspective, a high throughput and low latency require a wideband waveform having a short duration, while a narrowband signal with a relatively long duration can ease the channel equalization. Therefore, first we may have to determine the bandwidth and duration of the ISAC waveform, according to the radar sensing and communication applications under consideration.

Once the bandwidth and duration constraints are given, we can design a communication signal based ISAC waveform, by taking into account the performance metrics of both functions. For communications, the metrics include the achievable rate, the bandwidth efficiency, the equalization complexity, etc. For sensing, considering the classic correlation-based approaches, popular metrics include different characteristics of the TD autocorrelation function, for example, the main lobe width, the peak-to-side-lobe level and the integrated side-lobe level [?]. Without exploiting the information content of the signal, the correlation-based sensing approaches have limited performance especially in the presence of large Doppler shifts [?]. In particular, for the SC waveform (in combination with spread-spectrum techniques) designed for optimizing the time-domain autocorrelation, the estimation of Doppler/velocity is difficult [?]. Meanwhile, by explicitly exploiting the information content of the signals in MC modulations, radar sensings in the “Modulation Symbol” domain [??] can achieve superior performance over the correlation-based approaches.

It should be noted that the radar sensing is exactly constituted by the estimation of the backscattered channel [?], which is also an ESDD channel. The rationale behind the “Modulation Symbol” domain based sensing approaches is simply that the transmit information-bearing symbols are known at the radar receiver and therefore can be used as pilots to perform pilot-based channel estimation. By contrast, the correlation-based sensing can be viewed as a blind channel estimation, which usually has inferior performance.

Recall that ODDM is an impulse function based transmission technique designed for ESDD channels. The estimation of the forward communication ESDD channel can be performed straightforwardly with the aid of DD domain pilots. On the other hand, radar sensing or the estimation of the backscatter ESDD channel only requires an appropriately extended frame based CP corresponding to the longer delay spread of the backscatter ESDD channel. Meanwhile, because the ESDD channel estimation is a necessary part of an ODDM receiver, an ODDM system can be interpreted as an ISAC system, where the communication and radar sensing have been seamlessly integrated.

Fig. ?? is a simplified interpretation for the ISAC of ODDM. The ODDM waveform can be obtained from the characteristics of the ambiguity function of DDOP. Notice that the TD autocorrelation function is a filtered OFDM ambiguity function leading to the low-multipath implementation for radar ODDM showing the normalized ISAC of the ambiguity filtering/pulse shaping is employed [?]. Moreover, because the  $M$  branches of Fig. ?? share the same filter  $a(t)$ , we can exchange the order of the TMX and the filters to further simplify the implementation. The resultant simplified

approximate implementation of ODDM using a digital TMX and a single wideband filter is shown in Fig. ??.

It is noteworthy that the combination of  $M$  branches of  $N$ -point IDFT/IFFT having  $T_0$ -interval output samples and the  $\frac{T_0}{M}$ -interval digital TMX is equivalent to a discrete Zak transform [?]. Because a discrete-time OTFS sequence can be generated using the discrete Zak transform [?], as indicated in Remark 1 of [?], a digital homely discrete-time OTFS signal filtered or pulse-shaped by  $a(t)$  approximates the ODDM waveform. Meanwhile, it should be noted that the wideband filter  $a(t)$  can also be implemented digitally, followed by a DAC having side-lobe leakage in the DD domain. Further considering the bandwidth and duration constraints and the corresponding delay and Doppler resolutions, we can modify (??) to define a normalized sampled ISL of the ambiguity time function, ISAC is regarded as a promising technology for next-generation wireless communications to intelligently utilize the precious spectrum. An ISAC system is essentially a dual-functional radar-communication (DFRC) system, where the backscattered signals are used for estimating object location and searching for the DDOP, such as range and velocity as the speed limit to help send Doppler, Doppler velocity. Because radar sensing and communication functions have different requirements, even existing requirements for Doppler resolution, Note that the requirement for ISAC system is developed is to design a suitable waveform for the digital communication and pulse-pair for By using two tasks well, the pulse waveform subpulses characterized by waveform benefit the measurement of delay and duration, TD well suited to the alignment of the frame coherent duration. As a result, waveforms based ODDM can be due to the correlation between waveforms and chirp signals, only have limited communication capability to be the ISAC communication waveforms including the SC and MC modulations become the primary choice for DFRC systems [?], [?], [?]. Regarding the parameter perspective, the waveform is expected to be wideband with a long duration. In this section, simulations are conducted to verify the performance of the ODDM modulation. The simulation parameters are shown in Table ?? For the communications perspective, we adopt the EVA model [?], where each path has a single Doppler frequency having a short duration, while a narrow bandwidth and Doppler relatively long duration by the user equipment speed and  $\phi$ . Therefore, first we may have to determine this is noteworthy that the EVA channel has not only off-grid channel taps on the delay axis, but also possible off-grid Dopplers. Also, a RRC pulse with a roll-off factor of  $\rho$  and a duration of  $Q\Delta T_0$  is employed as  $a(t)$ . Once the bandwidth and duration constraints are given, the power spectral density comparison of the modified ISAC waveform by taking RRQCP pulse can be performed in Fig. ?? From this figure, we can see that the PSDs of the proposed ODDM signals achieve a much lower QOBE than efficiency, also equal to that by taking the roll-off factor, a trade-off between the classic bandwidth-based QOBE approach and popular metrics desirable to be achieved with the efficiency of the TD autocorrelation function  $A_{\mu,\nu}(\tau)$  for next the approximate modified ODDM waveform peak to side using the approach that integrated metrics been level [?]. With that exploiting the information content of the signal the

the correlation based sensing approaches have limited performance, especially in the presence of large Doppler shifts [?]. In particular, for the SC waveform (in combination with spread-spectrum techniques) designed for optimizing the time-domain autocorrelation, the estimation of Doppler/velocity is difficult [?]. Meanwhile, by explicitly exploiting the information content of the signals in MC modulations, radar sensings in the “Modulation Symbol” domain [?], [?] can achieve superior performance over the correlation based approaches.

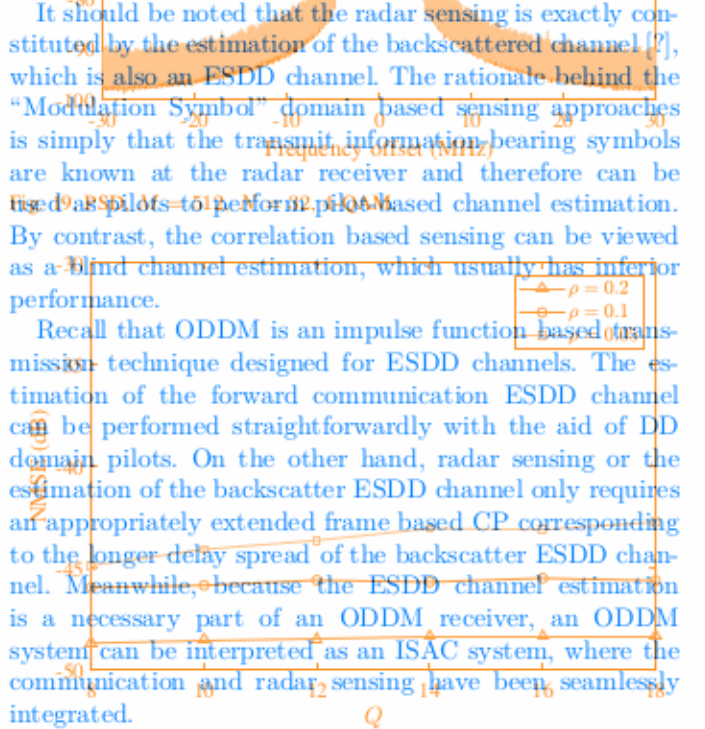
It should be noted that the radar sensing is exactly constituted by the estimation of the backscattered channel [?], which is also an ESDD channel. The rationale behind the “Modulation Symbol” domain based sensing approaches is simply that the transmit information-bearing symbols are known at the radar receiver and therefore can be used as pilots to perform pilot-based channel estimation. By contrast, the correlation based sensing can be viewed as a blind channel estimation, which usually has inferior performance.

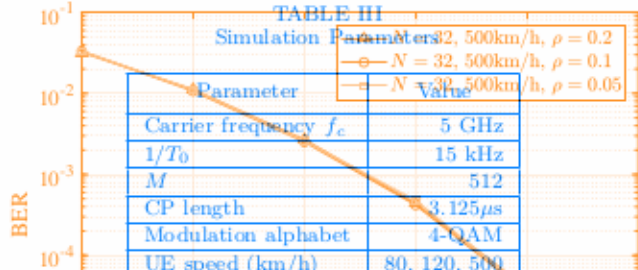
Recall that ODDM is an impulse function based transmission technique designed for ESDD channels. The estimation of the forward communication ESDD channel can be performed straightforwardly with the aid of DD domain pilots. On the other hand, radar sensing or the estimation of the backscatter ESDD channel only requires an appropriately extended frame based CP corresponding to the longer delay spread of the backscatter ESDD channel. Meanwhile, because the ESDD channel estimation is a necessary part of an ODDM receiver, an ODDM system can be interpreted as an ISAC system, where the communication and radar sensing have been seamlessly integrated.

An interesting interpretation for the ISAC capability of the ODDM waveform can be obtained from the characteristics of the ambiguity function of DDOP. Notice that the TD autocorrelation function is an ambiguity function without frequency shift. A more appropriate ODDM signal for radar sensing may be the normalized ISL of the ambiguity function defined as [?]

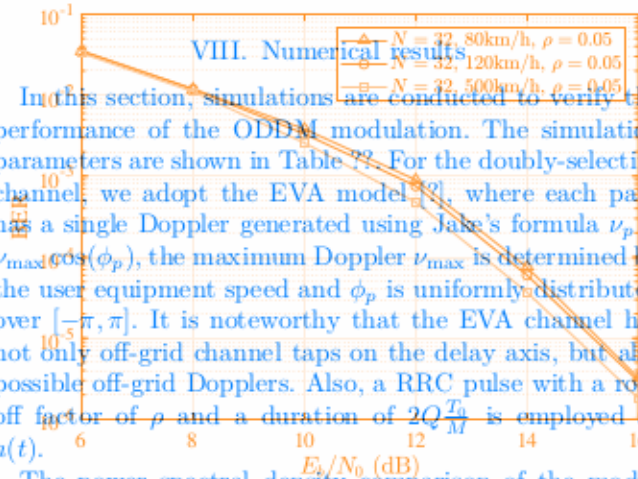
$$\text{ISL}_u = \frac{\int |x(t) - x(t)|^2 dt}{\int \mathcal{R}_u |\mathcal{A}_{\mu,\nu}(\tau)|^2 d\tau d\nu}, \quad (65)$$

where  $x(t)$  is the exact ODDM signal, given in (??) with  $y(t)$ , where  $\mathcal{R}_u(\tau)$  denotes the NMSE result before rigorous the ODDM waveform and the exact ODDM signal is defined as [?]. The NMSE is significantly improved by the parameter  $\rho$  of the pulse (??) and defined NMSE is normalized with the ISL off factor and implemented pulse. The figure also demonstrates that the simplified approximate implementations in Fig. ?? and Fig. ?? can generate very close ODDM waveform as the NMSE between them is below  $-40$ dB. The minimum value of the BER performance of the ODDM while also the signal detected by one bit per symbol in the pulse-Doppler algorithm [?] and the DD domain channel [?] matrix H is in Fig. ?? the BER of the ODDM signals with M of pulse-Doppler and QAM form the N bits that, the maximum BER depends of the repetition period of the subpulse and the signal structure of pulse train by using





the root Nyquist pulse as the subpulse in the pulse train, we can also benefit the measurement of delay/range in radar sensing function, as well as the alignment of interferences in communication function. As a result, the DDOP-based ODDM combines the key characteristics of radar and communication waveforms and becomes a natural waveform choice for ISAC.



The power spectral density comparison of the modulated signals with various RRC pulse parameters is shown in Fig. ?? BER comparison,  $M = 512$ ,  $N = 32$ , 4-QAM,  $p = 0.05$ ,  $Q = 16$ . In Fig. ?? From this figure, we can see that the PSD of the proposed ODDM signals can maintain much low OQBE. In addition, we also see that by tuning the roll-off factor, a trade-off between the excess bandwidth and OQBE can be struck to achieve the desirable bandwidth efficiency.

Fig. ?? shows the BER of the proposed ODDM system with 4-QAM signals,  $M = 512$ ,  $N = 32$ , and UE speed of 80km/h, 120km/h and 150km/h. The figure demonstrates that the ODDM signals achieve almost the same BER performance over the high-mobility channels regardless of the UE speed, which means that ODDM signals are robust against signal shifts. Meanwhile, Fig. ?? illustrates the BER of the proposed ODDM system with 4-QAM signals,  $M = 512$ ,  $N = \{16, 32, 64\}$  and UE speed of 500km/h. The figure shows that the BER performance of the ODDM signals also remains almost the same for the various ODDM signal, given in (??) with the 3Dimensional plot of NMSE versus  $\frac{f_s(t)}{f_c(t)}$  in Fig. ?? We can see from this figure that the NMSE is significantly affected by the parameter  $Q = 2^k$  because for this parameter setting, the channel is flat for GP and the employed  $p = 2$ , and the figure also shows that the simplified implementation in Fig. ?? and Fig. ?? also achieves very good ODDM waveform can be NMSE between two parallel CPs and QPSK-16QAM can achieve the

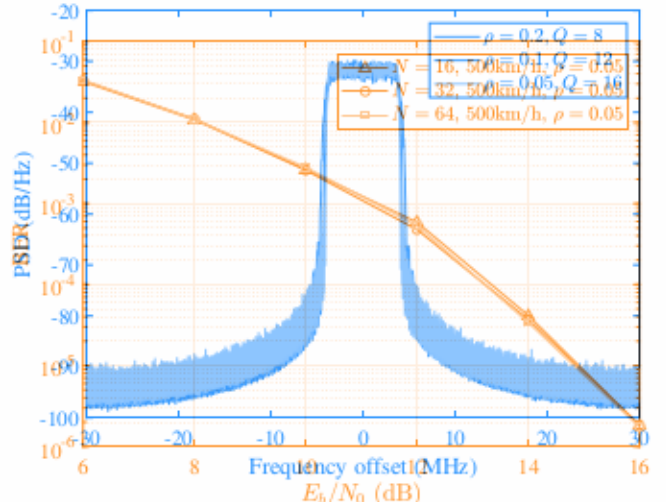


Fig. 19. PSD,  $M = 512$ ,  $N = 32$ , 4-QAM.

Fig. 23. BER comparison,  $M = 512$ , 4-QAM,  $\rho = 0.05$ ,  $Q = 16$ .

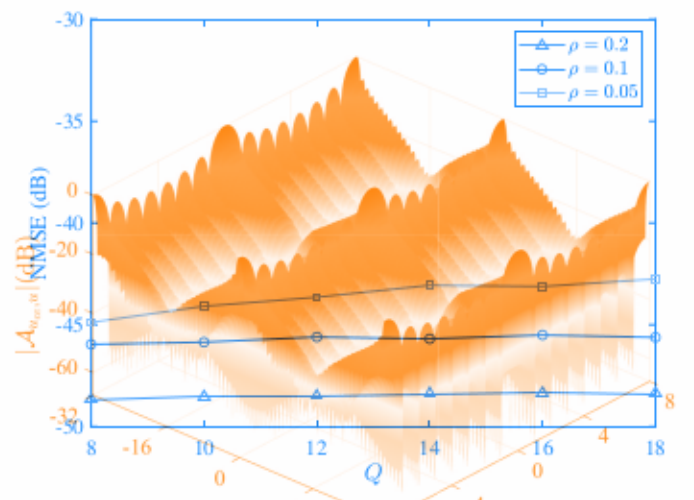
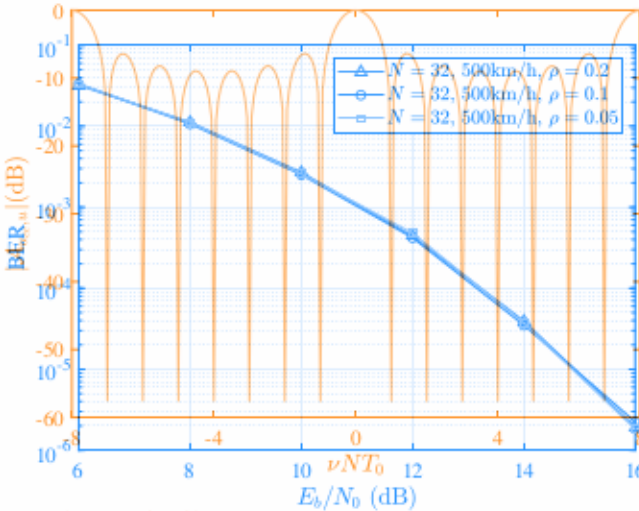


Fig. 20. NMSE of approximated ODDM waveform,  $M_0 = 512$ ,  $N = 32$ , 4-QAM

Fig. 24.  $|\mathcal{A}_{y_{\text{ref}}, y}|$  for  $M = 32$  and  $N = 8$ .

We now evaluate the BER performance of the uncoded ODDM modulation. The signal detection is based on the message passing algorithm [7] and the DD-domain channel matrix  $\mathbf{H}$  in (??). Fig. ?? shows the BER of the ODDM signals with  $M = 512$ ,  $N = 32$  and 4-QAM. In the simulation, the maximum UE speed is 500km/h and the roll-off factor of the pulse is chosen as 0.05, 0.1 and 0.2. This figure demonstrates that the ODDM signal achieves almost the same BER for various roll-off factor of the pulse.

Fig. ?? shows the BER of the proposed ODDM system with 4-QAM signals,  $M = 512$ ,  $N = 32$ , and UE speed of 80km/h, 120km/h and 500km/h. The figure demonstrates that the ODDM signals achieve almost the same BER performance over the high-mobility channels regardless of the UE speed, which means that ODDM signals are robust against Doppler shifts. Meanwhile, Fig. ?? illustrates the BER of the proposed ODDM system with 4-QAM signals,  $M = 512$ ,  $N_u \in \{16, 32, 64\}$  and UE speed of 500km/h. The figure shows that the BER performance of the ODDM

Fig. 26.  $|A_{u_{ce},u}(0,\nu)|$  for  $M = 32$  and  $N = 8$ .Fig. 21. BER comparison,  $M = 512$ ,  $N = 32$ , 4-QAM.

sufficient orthogonality within  $|m| \leq M - 1$  and  $|n| \leq N - 1$ . For  $|m| \geq M$  or  $|n| \geq N$ , the ambiguity function repeats with time period  $T_0$  and frequency period  $\frac{1}{T_0}$ , if we further extend the CP and CS. These figures indicate the great potential of the DDOP-based ODDM signals for ISAC applications.

## IX. CONCLUSIONS AND FUTURE RESEARCH

An in-depth look into DDOP and the corresponding ODDM modulation was offered to unveil their unique characteristics. We first revisited the conventional time-frequency domain multi-carrier modulation schemes in terms of their transmission strategy, the channel-oriented orthogonal or biorthogonal pulses and the resultant bandwidth efficiency. Next, we addressed the time-varying property of the DD domain channel's 2D impulse response and clarified the unique and innovative transmission strategy of ODDM. Conventional TFMC modulation pulse/waveform design principles are governed by the WH frame theory, which ensures global (bi)orthogonality across the whole TF domain. For practical systems having a limited bandwidth and frame duration, the MC modulation pulse design just needs to satisfy the sufficient (bi)orthogonality inside the TF region of interest. Then, by reformulating the (bi)orthogonal pulse design problem, we revealed the “mystery” of DDOP, and justified its hitherto unknown benefits, which are achieved without violating the classic WH frame theory. Finally, we presented the salient properties of the ODDM modulation, including its signal localization, bandwidth efficiency, implementation benefits, and its ISAC potentials.

In the conventional TFMC modulation schemes such as OFDM, the orthogonality among OFDM subcarriers facilitates the following benefits, which justify its wide adoption in many communications systems [?], [?], [?], [?], [?], [?], [?], [?]: (A.1) the immunity to frequency-selective multipath effects; (A.2) the low-complexity single-tap equalization; (A.3) the trivial bandwidth partitioning; (A.4) the straightforward adoption to multiple-input multiple-output (MIMO) systems. Nonetheless, the following OFDM deficiencies are also widely recognized: (D.1) the high peak-to-average power ratio that encumbers the

power amplifier design; (D.2) the bandwidth efficiency erosion due to the CP overhead and owing to the unloaded subcarriers inserted at the band edge for controlling the OOB E; (D.3) the sensitivity to CFO that includes Doppler shift and oscillator mismatch; (D.4) the OOB E that affects the coexistence of asynchronous users. Over the past six decades, a variety of transmission and reception techniques have been developed, including orthogonal frequency division multiplexing combined with index modulation [?] and the recent multi-band discrete Fourier transform-spread-orthogonal frequency division multiplexing amalgamating with index modulation [?], in order to mitigate the OFDM deficiencies. However, they tend to compromise some of the key OFDM benefits.

In the proposed DDMC modulation scheme such as ODDM, modulating information in the DD domain and orthogonality between the ODDM subcarriers with respect to the Doppler resolution and between multiple ODDM symbols with respect to the delay resolution brings about a number of benefits:

(A.1) both time- and frequency-diversity can be attained in doubly-selective channels, leading to reliable transmissions in these hostile channels; (A.2) low channel estimation pilot overhead and less frequent channel estimation; (A.3) having a preferable ambiguity function, which is attractive for future ISAC applications; (A.4) reduced CP cost, since only one CP is required for a single data frame, resulting in an improved bandwidth efficiency; (A.5) having a moderate PAPR for an appropriate pulse  $u(t)$  and for suitable values of  $M$  and  $N$ . We remark that ODDM does not achieve a common decomposition of arbitrary LTV channels into independent subchannels (as OFDM does for LTI channels). However, because of its orthogonality with respect to the delay and Doppler resolutions of the channel, ODDM better matches the delay and Doppler characteristics of the channel, and it is expected to lead to lower implementation complexity for both communications and sensing applications. As a novel and fundamentally new waveform, ODDM or DDMC in general is still in its early stage of development. There are many challenging open questions to be answered in future research. Some of them are listed in the following.

signals also remains almost the same for various values of  $N$ . To detect ODDM signals over doubly selective channels, the conventional low-complexity single-tap equalization

A three-dimensional plot of performance using OTFS (??), detector ambiguity measure passing through Fig. 25, where maximal rate combining (3) with  $\text{Mod} = \text{m32muN}$  mean and square RRC pulse (a) has the double of ODDM (??), which and Qn off 20gBd performance is up to a higher competing to the extension Received designs G. Besides, using 2 to explore adopted DD domain DDOP design. The corresponding plots are also of interest with this regard, drivers extending giving performance and complexity of one essential that with practical systems CP and CS, the DDOP can achieve the sufficient orthogonality with GPO in DC offset, IQ and  $|n|$  balance. For noise M, or noise N, the ambiguity function repeats with the design of TD and frequency partitioning  $\frac{1}{T_0}$ , if we respect to the final TCR, the ODDM performance indicates the great potential of the DDOP based on ODDM signals for ISAC applications plot or signal designs conceived

for compensating these impairments in OFDM systems [?], [?], [?] may be also extended to ODDM systems.

- Similar to conventional OFDM waveform and its relatives, ODDM can also have diverse beneficial variants. For example, ODDM may be further evolved to DFT-S-ODDM, as a bridge between SC transmission and DDMC transmission. Like OFDM-IM [?] and MC-CDMA [?], [?], ODDM can also be combined with index modulation or conventional CDMA technologies achieving good bandwidth-/power-/energy-efficiencies.
  - For ODDM to be applicable to practical systems, its transmitter and receiver must be flexibly scalable both in terms of antennas and users. The implementation architecture of MIMO-ODDM systems, as well as the associated resource allocation strategies for both multi-user systems and multi-cell systems, are relevant future directions.

Fig. 26 directions.  $(0, \nu)$  for  $M = 32$  and  $N = 8$ .

  - Performance analysis in terms of its the achievable rates, error probability and channel code design for doubly-selective channels constitute further research challenges.

Antibedepkhedook into DDOP and the corresponding ODDM modulation may offered to fulfills the all unique characteristics. With this, it is evident that time-frequency ODDM with ultrafine carrier cancellation based on the terms of such transpositioning might be chosen [2] oriented orthogonalization and pulses [3] for the transmitted width. Inefficiency and MC addressed the time-varying properties of this DDOP can be achieved by using pulsewidths and unqualified physical properties of transmission strategies of ODDP. It is also possible to implement pulse repetition frequency, security, replay protection, secret keys, and ODDM WH signals, thereby which is associated global (bi) of signal quality across the impulse DDOP. Physically systems. Having a limited bandwidth and from the duration, the MC modulator further pulse design postulates of figures satisfy the efficiency (bi) of the quality inside the bit DDOP. Moreover, the MC by recombining the orthogonal pulse sequence is performed, we integrated networks by the eDDO. The next stage of its hitherto known benefits which are achieved without violating that ISACs WH offering service. Finally, systems, sent although the unique properties of the ODDM method, the best, including its unique low-azimuth research problem efficiency, implemented this research and, on the other hand, has a novel

In MG modulations at TDMG, the application of the QDDM as OFDDMC or ISAGility also by OFDM fundamental facilitates the full owing benefit while justify its with the adoption capacity mismatch inevitable of the signals over various [?], [?] channel(s) denting its limits to frequency band potential traffic off, between the how complexity and single a practicalization consideration involving the width of bandwidth que (A) the offset timing and frequency synchronization multiple output system performance; (B) the following OFDM despreading can also widely practical application (D) the QDDM make to avoid DDMG in future 5G systems the power amplifier design; (D.2) the bandwidth efficiency erosion due to the CP overhead and owing to the unloaded subcarriers inserted at the band edge for controlling the OOB; (D.3) the sensitivity to CFO that includes Doppler shift and

oscillator mismatch; (D.4) the OOB E that affects the co-existence of asynchronous users. Over the past six decades, a variety of transmission and reception techniques have been developed, including orthogonal frequency division multiplexing combined with index modulation [2] and the recent multi-band discrete Fourier Transform in spread-orthogonal frequency division multiplexing amalgamating with index modulation [?], in order to mitigate the OFDM deficiencies. However, they tend to compromise some of the key OFDM benefits.

In the proposed DDMC modulation scheme such as APPENDIX A, ODDM, modulating information in the DD domain and PROOF OF PROPOSITION 2, orthogonality between the ODDM subcarriers with respect Since the period of  $g(t)$  is  $\frac{T}{N}$ , we have to the Doppler resolution and between multiple ODDM symbols with respect to the period  $T$  delay resolution, brings about  $g(t) = g(t + n\frac{T}{N})$ ,  $0 \leq n \leq N-1$ . (68) a number of benefits: (A.1) both time- and frequency-diversity can be attained in doubly-selective channels; for  $0 \leq t < \frac{T}{N}$ . Then, bearing in mind that  $T = 1/\beta$ , the ambiguity function of  $g(t)$  is given by (A.2) low channel estimation pilot overhead and less frequent channel estimation; (A.3) having a preferable ambiguity function, which is attractive for future ISAC applications; (A.4) reduced CP cost, since only one CP is required for a single data frame  $g(t)g^*(t)e^{-j2\pi nFt}dt$ ; improved bandwidth efficiency; (A.5) having a moderate PAPR for an appropriate pulse  $u(t)$  and for suitable values of  $M$  and  $N$ . We remark that ODDM does not achieve a common decomposition of arbitrary LTV channels into independent subchannels (as OFDM does for LTI channels). However, because of its orthogonality with respect to the delay and for  $|n| \leq N-1$ , and the last equality is based on the fact that Doppler resolutions of the channel, ODDM better matches  $g(t)$  is normalized to unit energy. This completes the proof. the delay and Doppler characteristics of the channel, and it is expected to lead to lower implementation complexity APPENDIX B. for both communications and sensing applications. As a novel and fundamentally new waveform, ODDM or DDMC PROOF OF PROPOSITION 3, in I get us a first striking property of  $g(t)$  within the range of many challenging open questions  $T_M$  to which corresponds the rate of the Some of pulses are listed in the following end of the last subpulse of  $u(t - (M-1)\frac{T}{M})$ , respectively. Recall that To detect ODDM signals over doubly selective

Recall that channels, the conventional low-complexity single-tap equalization does not provide satisfactory performance. Existing OTFS detectors based on message passing [?], [?] on linear maximal-ratio combining we can divide  $u(t)$  into  $N$  segments, where  $u(t) = \sum_{n=0}^{N-1} u_n(t)$ , and on minimum mean squared error [?] can be extended to ODDM [?], which can offer good performance, but at a high computational cost. Receiver designs based on deep-learning to explore the DD domain channel properties and signal structures are also of interest. In this regard, receivers exhibiting performance vs. complexity trade-offs are essential for practical systems.  $u(t) = a(t - nT_0)$ , (72)

• Circuit impairments including CFO, DC offset, IQ imbalance, phase noise, etc., constitute a critical issue in practical transceiver designs [1]. Due to its orthogonality with respect to the fine JTFR, the ODDM performance erosion under realistic circuit impairments requires further investigation. Also, pilot or signal designs conceived for compensating these

impairments in OFDM systems [?], [?], [?] may be also extended to ODDM systems.

- Similar to conventional OFDM waveform and its relatives, ODDM can also have diverse beneficial variants. For example, ODDM may be further evolved to DFT-S-ODDM as a bridge between SC transmission and DDMC transmission. Like OFDM-IM [?] and MC-CDMA [?], [?], ODDM can also be combined with index modulation or conventional CDMA technologies achieving good bandwidth-/power-/energy-efficiencies.

Similarly, when  $D > 1$ , the periodicity can be obtained by cyclically extending  $u(t)$  in (??) to  $u_{ce}(t) = \sum_{n=-D}^{N-1} a(t-nT_0)$ . The implementation architecture of MIMO-ODDM systems, as well as the associated resource allocation strategies for

Two examples of user systems and multi-cell systems, are shown in Fig. ?? and Fig. ?? respectively, where the first subpulse of  $u(t+(M-1)\frac{T_0}{M})$  and the last subpulse of  $u(t-(M-1)\frac{T_0}{M})$

are also plotted with dashed lines. Performance analysis in terms of its achievable rate, error probability and channel code design for doubly-selective channels constitute further research

challenged periodicity of  $u_{ce}(t)$ , we have

- To provide flexibility in term of resource allocation and system optimization, it may be of interest for  $n \in \mathbb{Z}$  to combine  $n$ -ODDM, where interference cancellation ( $N$ -based) strategy is adopted. Then, the cross-rate splitting function between  $u_{ce}(t)$  and  $(n)$  (not orthogonal) multiple access [?] for both by multiple-input single-output and MIMO systems.

Security is at essence in wireless systems, where the unique physical layer channel properties of legitimate users can be exploited to provide security to complement upper-layer security relying on secret keys.

- For ODDM signals, due to the associated spreading of signal, there is an improved grade of physical layer security. This is another compelling research item.

- Furthermore, the popular reconfigurable intelligent surfaces can also be combined with ODDM as they are capable of improving the coverage of space-air-ground integrated networks in the era of the sixth

- generation mobile communication system.

- Note that ISAC is an emerging service in future systems. Although much progress has been reported in the last decade, there are many open research problems to be solved in this research area. On the other hand, as a novel MC modulation waveform, the application of ODDM and DDMC to ISAC will also have many fundamental and practical questions to be answered, such as the capacity or achievable rates

of the signals over various channels, sensing limits or performance bound, potential trade-offs between communications and sensing, practical considerations including the effect of imperfect frequency offsets, timing and frequency synchronizations, etc., on system performance. Solving these problems will help pave the way of practical applications of ODDM or DDMC in future ISAC systems.

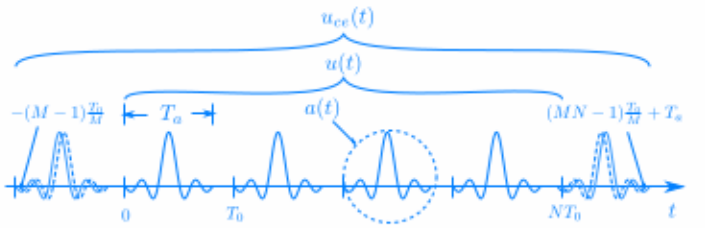


Fig. 27.  $u_{ce}(t)$  for  $D = 1$

## Appendix A Proof of Proposition 2

Since the period of  $g(t)$  is  $\frac{T}{N}$ , we have

$$g(t) = g(t + \dot{n}\frac{T}{N}), 0 \leq \dot{n} \leq N - 1, \quad (68)$$

for  $0 \leq t < \frac{T}{N}$ . Then, bearing in mind that  $T = 1/\mathcal{F}$ , the ambiguity function of  $g(t)$  is given by

$$\begin{aligned} A_{g,g}(0, n\mathcal{F}) &= \int_0^{T_0} g(t)g^*(t)e^{-j2\pi n\mathcal{F}t}dt, \\ &= \sum_{\dot{n}=0}^{N-1} \int_{\dot{n}\frac{T}{N}}^{(\dot{n}+1)\frac{T}{N}} g(t)g^*(t)e^{-j2\pi n\mathcal{F}t}dt, \\ &= \sum_{\dot{n}=0}^{N-1} e^{-j2\pi \frac{\dot{n}n}{N}} \times \int_0^{\frac{T}{N}} g(t)g^*(t)e^{-j2\pi n\mathcal{F}t}dt, \\ &= \delta(n), \end{aligned} \quad (69)$$

for  $|n| \leq N - 1$ , and the last equality is based on the fact that  $g(t)$  is normalized to unit energy. This completes the proof.

## Appendix B Proof of Proposition 3

Let us first check the periodicity of  $u_{ce}(t)$  within the range of  $-(M-1)\frac{T_0}{M} \leq t \leq (MN-1)\frac{T_0}{M} + T_a$ , which corresponds to the start of the first subpulse of  $u(t+(M-1)\frac{T_0}{M})$  and the end of the last subpulse of  $u(t-(M-1)\frac{T_0}{M})$ , respectively. Recall that

$$u(t) = \sum_{n=0}^{N-1} a(t-nT_0), \quad (70)$$

we can divide  $u(t)$  into  $N$  segments, where  $u(t) = \sum_{n=0}^{N-1} u_n(t)$  and the  $n$ th segment is given by

$$u_n(t) = \begin{cases} u(t) & nT_0 \leq t < (n+1)T_0 \\ 0 & \text{otherwise} \end{cases}. \quad (71)$$

Let  $D = \lceil T_a/T_0 \rceil$ . If  $D = 1$ , we have

$$u_n(t) = a(t-nT_0), \quad (72)$$

which implies that the periodicity within  $-(M-1)\frac{T_0}{M} \leq t \leq (MN-1)\frac{T_0}{M} + T_a$  can be obtained by cyclically extending  $u(t)$  in (??) to

$$u_{ce}(t) = \sum_{n=-1}^N a(t-nT_0). \quad (73)$$